(2)

THE OHIO STATE UNIVERSITY

Fundamental Research on Erosion in Magnetoplasmadynamic Thrusters

V. V. Subramaniam
Department of Mechanical Engineering

Air Force Office of Scientific Research
Bolling Air Force Base, D.C. 20332-6448

Grant No. AFOSR-87-0360
Annual Technical Report

July 1991

REPORT DOCUMENTATION PAGE

1a. REPORT SECURITY CLASSIFICATION Unclassified	1b. RESTRICTIVE MARKINGS
2a. SECURITY CLASSIFICATION AUTHORITY	3. DISTRIBUTION / AVAILABILITY OF REPORT Approved for public release; distribution is unlimited
2b. DECLASSIFICATION / DOWNGRADING SCHEDULE	
4. PERFORMING ORGANIZATION REPORT NUMBER(S) RF719942/766307	5. MONITORING ORGANIZATION REPORT NUMBER(S) AFOSR-TR- 91 0891
6a. NAME OF PERFORMING ORGANIZATION The Ohio State University Mechanical Engineering Dept. 6b. OFFICE SYMBOL (If applicable)	7a. NAME OF MONITORING ORGANIZATION AFOSR/NA
6c. ADDRESS (City, State, and ZIP Code) The Ohio State University Office of Sponsored Programs 1960 Kenny Road; Columbus, Ohio 43210	7b. ADDRESS (City, State, and ZIP Code) Building 410, Bolling AFB DC 20332-6448
8a. NAME OF FUNDING / SPONSORING ORGANIZATION AFOSR/NA 8b. OFFICE SYMBOL (If applicable)	9. PROCUREMENT INSTRUMENT IDENTIFICATION NUMBER AFOSR-87-0360
8c. ADDRESS (City, State, and ZIP Code) Building 410, Bolling AFB DC 20332-6448	10. SOURCE OF FUNDING NUMBERS PROGRAM ELEMENT NO. 61102F; PROJECT NO. 2308; TASK NO A1; WORK UNIT ACCESSION NO.

11. TITLE (Include Security Classification)
(U) Annual Technical Report on Fundamental Research on Erosion in Magnetoplasmadynamic Thrusters

12. PERSONAL AUTHOR(S)
V. V. Subramaniam

13a. TYPE OF REPORT	13b. TIME COVERED	14. DATE OF REPORT (Year, Month, Day)	15. PAGE COUNT
Annual Tech. Report	FROM 10/90 TO 10/91	1991/7/1	

16. SUPPLEMENTARY NOTATION

17 COSATI CODES			18. SUBJECT TERMS (Continue on reverse if necessary and identify by block number)
FIELD	GROUP	SUB-GROUP	MPD Thruster, Electrode Processes, Erosion, Electrode-Plasma Interactions.

19. ABSTRACT (Continue on reverse if necessary and identify by block number)

Significant developments have been made toward a comprehensive theory of Onset and erosion in steady state self-field MPD thrusters. The Back-EMF Onset theory predicts that the middle region of the cathode (i.e. away from the inlet and exit) and the near inlet and exit regions of the anode are susceptible to severe erosion. This erosion occurs due to excessive electron bombardment at a critical value of the local sheath voltage drop (or current density). Furthermore, this theory predicts that the regions of potential and magnetic field oscillations observed at Onset occur predominantly in the high current density regions of the cathode (i.e. near the inlet and exit regions) and in the low current density regions at the anode. Past experimental observations at Princeton, and recent observations from Stuttgart support the predictions of this theory. The research described here provides a summary of the accomplishments and progress made during the final year under grant AFOSR-87-0360.

20. DISTRIBUTION / AVAILABILITY OF ABSTRACT ☒ UNCLASSIFIED/UNLIMITED ☒ SAME AS RPT ☐ DTIC USERS	21. ABSTRACT SECURITY CLASSIFICATION Unclassified
22a. NAME OF RESPONSIBLE INDIVIDUAL Dr. Mitat Birkan	22b. TELEPHONE (Include Area Code) (202) 767-4938 22c. OFFICE SYMBOL AFOSR/NA

DD FORM 1473, 84 MAR 83 APR edition may be used until exhausted. All other editions are obsolete.

THE OHIO STATE UNIVERSITY

Fundamental Research on Erosion in Magnetoplasmadynamic Thrusters

V. V. Subramaniam
Department of Mechanical Engineering

Air Force Office of Scientific Research
Bolling Air Force Base, D.C. 20332-6448

Grant No. AFOSR-87-0360
Annual Technical Report
RF Project No. 766307/719942

July 1991

Table of Contents

Fundamental Research on Erosion in Magnetoplasmadynamic Thrusters

Grant No AFOSR-87-0360

Annual Technical Report
(1989-1990)

V. V. Subramaniam
Department of Mechanical Engineering
The Ohio State University
Columbus, Ohio 43210

1. Introduction

The Back-EMF theory of Onset has been refined and expanded to enable prediction of erosion rates for steady state, self-field MPD thrusters[1]. This theory is capable of explaining both the observed oscillations as well as the increased erosion at Onset. This represents the first time that the plasma discharge and electrode processes have been coupled. Recent experiments at the Institut fur Rahmfahrtsysteme at Stuttgart reveal cathode damage at precisely the same location as that predicted by this theory[2]. The research described in this report provides a summary of the accomplishments and progress made during the three years and specifically during the final year under this grant AFOSR-87-0360.

2. Research Objectives

The purpose of this research is to understand and quantify the mechanisms responsible for evaporative erosion in steady state magnetoplasmadynamic (MPD) thrusters. This is an important step in being able to predict thruster lifetimes. Erosion processes depend on a

complex coupling between plasma discharge characteristics, plasma-wall interactions, and electrode phenomena. In particular, erosion rates depend on whether the current conduction is through localized spots, or via a diffuse (distributed) mode. Spots are detrimental to the electrode material because of their high erosion rates. Therefore, it is important to understand how and under what conditions they may be formed, and exactly when diffuse mode behavior ends. Much of the focus of this research is on the cathode. The following overall objectives were set for this research effort: (1) to identify the limits of steady state diffuse mode electrode operation, (2) to identify the mechanisms responsible for limiting the diffuse mode, (3) to model the thermal response of the cathode at steady state, thereby enabling the prediction of surface temperatures and erosion rates due to evaporation, and (4) to enable prediction of the temporal thermal behavior of the cathode. Although no transient model of the bulk plasma flow in the MPD thruster exists presently, it should be forthcoming in the near future.

3. Status of the Research Effort

This section describes the highlights of the research during the final year of this grant. A more detailed discussion can be found in the appendices as well as in the references at the end of this report.

The Back-EMF theory was first formulated within the context of frozen, fully ionized channel flow in the MPD thruster[3]. It was found that MPD channel flow is parametrized by a non-dimensional parameter $S^* = B^{*2}/\mu_o F a^*$, called the Magnetic Force Number. S^* is defined with respect to quantities evaluated at the magnetogasdynamic sonic point (i.e. where M*=1), where B* is the magnetic induction, μ_o is the permeability of free space, F is the mass flux, and a* is the frozen speed of sound at the sonic point. S* may be interpreted as the ratio of magnetic pressure to kinetic energy density. Careful analysis of MPD channel flow revealed that:

(1) S* is related to the experimentally measured Onset parameter $J^2/\dot{m}$,

(2) fundamental limits exist on S* and hence on $J^2/\dot{m}$ for supersonic flow to exit the MPD channel, and

(3) Onset limits could be derived from first principles, in agreement with the experiments of Malliaris et. al.[4].

Incorporation of finite rate ionization and recombination did not alter these results, but an explicit analytical closed form expression for the limits on S* could not be found[5]. However, the numerically calculated Onset limit predicted by this theory agreed with quasi-steady experiments in straight coaxial thrusters[6]. The Onset limit predicted by this theory was related to excessive values of the Back-EMF which occur at high values of the total current for a given mass flow and geometry. This steady, quasi-one dimensional flow model provides variations of the important quantities (number densities, current density, temperature, velocity, ionization fraction, and magnetic induction) versus distance along the channel. This is done for a given mass flow rate, geometry, and total current.

The plasma flow and electrode processes in the MPD thruster are intimately coupled. A first attempt at treating this complex coupling consisted of using the axial profiles generated by the quasi-one dimensional model as boundary conditions for a two-temperature model of the electrode-adjacent boundary layer flow[7]. The boundary layer model provided distributions of heavy particle temperature, ionization fraction, and number densities in the direction transverse (i.e. radial) to the electrodes. Two important outcomes of this boundary layer theory were (a) that the heavy particle conductive heat flux was negligible compared to charged particle bombardment of the electrodes, and (b) that the highly viscous MPD boundary layer flow produces a maximum in the transverse heavy particle temperature distribution somewhere within the boundary layer well away from the core flow and the electrode surfaces. The boundary layer theory provided important boundary conditions for analyses of the sheath regions near the cathode and anode[8,9]. Analyses of the sheaths provided the final set of boundary conditions for thermal analyses of the electrodes[10,11]. These simple sheath models revealed several remarkable phenomena:

(1) Stable, diffuse mode behavior would transition into the spot mode at a critical value of the *sheath voltage drop*.

(2) This diffuse to spot transition was caused by a thermal runaway due to excessive *electron bombardment*.

(3) The thermal runaway was found to occur in the low current density regions of the cathode and the high current density regions of the anode.

(4) As the total current to the thruster is increased for a given mass flow and geometry, the current density profile along the thruster length reaches a minimum (due to excessive Back-EMF) in the middle while reaching local maxima at the inlet and exit.

(5) The regions of the anode closest to the inlet and exit of the thruster are thus at greatest risk in terms of erosion, while the middle region of the cathode is susceptible to erosion at a critical value of the current.

(6) The present theory also predicts that unstable voltage and electric field oscillations may occur at the high current density regions (i.e. near inlet and exit regions) of the cathode. These oscillations may be triggered by the energetic electrons emitted by the cathode surface interacting with the relatively slower plasma electrons (classical two-stream instability). Hence, the regions of greatest erosion are predicted *not* necessarily to occur in the regions of greatest oscillations.

Recently, there were two reports of tests conducted at Stuttgart on high power, steady state MPD thrusters[2]. These tests showed that in the two different geometries tested(one with a flared anode and the other with a straight anode), severe damage was encountered at the respective cathodes. In fact, the cathodes appear to have exploded from within (see Fig. 1). This damage occured at 6500 A for the flared anode (DT1 thruster) and at 8000 A for the straight coaxial ZT1 thruster. The Back-EMF theory of Onset not only correctly predicted these current limits but also predicted the temperature profiles shown in Fig. 2. As expected the centerline cathode temperatures far exceed the cathode surface temperatures at the Onset limit. Furthermore at the predicted Onset limit, the interior temperature exceeds the melting temperature. When this occurs, pressure builds up inside the cathode driving crack propagation and promoting fissures. Although the Back-EMF theory correctly predicts this Onset and damage limit, it cannot describe the events after the damage and melting have begun to occur.

In summary, the simple models developed thus far enable the designer to use quick tools for performance studies and design evaluations. Efforts are underway to develop quantitatively accurate predictions of the flow field in straight coaxial thrusters (2D axisymmetric simulations). Accurate models are still needed of the electrode pre-sheath regions where the prediction of ionization fraction is important. Specifically, research is underway to examine the combined effects of trapping of resonance radiation and ionization of excited species by electrons emitted from the electrodes.

4. Personnel

V. V. Subramaniam, principal investigator

J. W. Rich, co-investigator

G. Lefever-Button, Undergraduate/Graduate Student

J. Rebello, Graduate Student

V. Babu, Graduate Student

References

(1) V. V. Subramaniam, AFOSR annual technical report, AFOSR-87-0360, October 7, 1988.

(2) M. Auweter-Kurtz, B. Glocker, H. Kurtz, O. Loesener, H. O. Schrade, N. Tubanos, T. Wegmann, D. Willer, and J. Polk, "Cathode Phenomena in Plasma Thrusters", AIAA paper 90-2662, presented at the AIAA/DGLR/JSASS 21st International Electric Propulsion Conference, Orlando, Florida, July 18-20, 1990.

(3) J. L. Lawless, and V. V. Subramaniam, "Theory of Onset in Magnetoplasmadynamic Thrusters", *J. Propulsion & Power*, Vol. 3, No. 2, pp. 121-127, March-April 1987.

(4) A. C. Malliaris, R. R. John, R. L. Garrison, and D. R. Libby, "Performance of Quasi-Steady MPD Thrusters at High Powers", *AIAA Journal*, Vol. 10, No. 2, February 1972.

(5) V. V. Subramaniam, and J. L. Lawless, "Onset in Magnetoplasmadynamic Thrusters with Finite Rate Ionization", *J. Propulsion & Power*, Vol. 4, No. 6, pp. 526-532, November-December 1988.

(6) D. Q. King, *Magnetoplasmadynamic Channel Flow for Design of Coaxial MPD MPD Thrusters*, Ph.D. Dissertation, Princeton University, December 1981.

(7) V. V. Subramaniam, and J. L. Lawless, "Electrode-Adjacent Boundary Layer Flow in Magnetoplsmadynamic Thrusters", *Phys. Fluids*, Vol. 31, No. 1, pp. 201-209, January 1988.

(8) V. V. Subramaniam, K. S. Hoyer, and J. L. Lawless, "Limits on Steady Diffuse Mode Operation of the Cathode in Magnetoplasmadynamic Thrusters", *AIAA J. Propulsion & Power*, in press. See Appendix A for the preprint.

(9) V. V. Subramaniam, and J. L. Lawless, "Thermal Instabilities of the Anode in an MPD Thruster", *AIAA J. Propulsion & Power*, Vol. 6, No. 2, pp. 221-224, March-April 1990.

(10) K. S. Hoyer, *Steady-State Diffuse Mode Operation of the Cathode in a Magnetoplasmadynamic Thruster*, M. S. Thesis, The Ohio State University, June 1989.

(11) V. V. Subramaniam, "Onset and Erosion in Self-Field MPD Thrusters", AIAA paper 91-021, to be presented at the AIDAA/AIAA/DGLR/JSASS 22nd International Electric Propulsion Conference, Viareggio, Italy, October 14-17, 1991.

5. Interactions

The following papers and publications have resulted thus far from this grant:

(1) V. V. Subramaniam, K. S. Hoyer, and J. L. Lawless, "Limits on Steady Diffuse Mode Operation of the Cathode in Magnetoplasmadynamic Thrusters", *AIAA J. Propulsion & Power*, in press. See Appendix A for the preprint.

(2) V. V. Subramaniam, and J. L. Lawless, "Thermal Instabilities of the Anode in an MPD Thruster", *AIAA J. Propulsion & Power*, Vol. 6, No. 2, pp. 221-224, March-April 1990.

(3) K. S. Hoyer, *Steady-State Diffuse Mode Operation of the Cathode in a Magnetoplasmadynamic Thruster*, M. S. Thesis, The Ohio State University, June 1989.

(4) V. V. Subramaniam, "Onset and Erosion in Self-Field MPD Thrusters", AIAA paper 91-021, to be presented at the AIDAA/AIAA/DGLR/JSASS 22nd International Electric Propulsion Conference, Viareggio, Italy, October 14-17, 1991.

(5) G. Lefever-Button, *Quasi One-Dimensional Ionizing Supersonic Flow in a Magnetoplasmadynamic Thruster*, Undergraduate Honors Thesis, The Ohio State University, July 1990.

(6) G. Lefever-Button, and V. V. Subramaniam, "Quasi-One-Dimensional MPD Flow", AIAA paper to be presented at the AIDAA/AIAA/DGLR/JSASS 22nd International Electric Propulsion Conference, Viareggio, Italy, October 14-17, 1991.

(7) V. Babu, V. V. Subramaniam, and G. Lefever-Button, "A Two-Dimensional Axisymmetric Numerical Model of Frozen Flow in Self-Field MPD Thrusters", AIAA paper 91-090, to be presented at the AIDAA/AIAA/DGLR/JSASS 22nd International Electric Propulsion Conference, Viareggio, Italy, October 14-17, 1991.

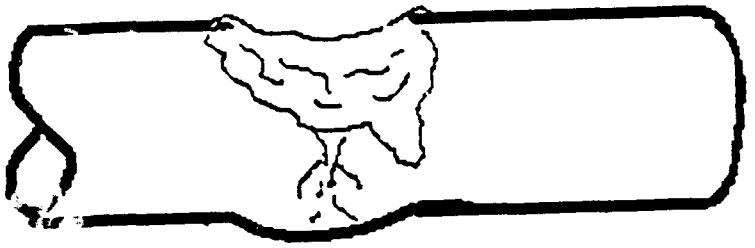

Fig.1:Schematic of the type of damage sustained by the DT2 and ZT1 thrusters after sustained steady state operation at 6500 A and 8000 A respectively. The total argon propellant flow reported was 2 g/s. For further details, please see reference [11].

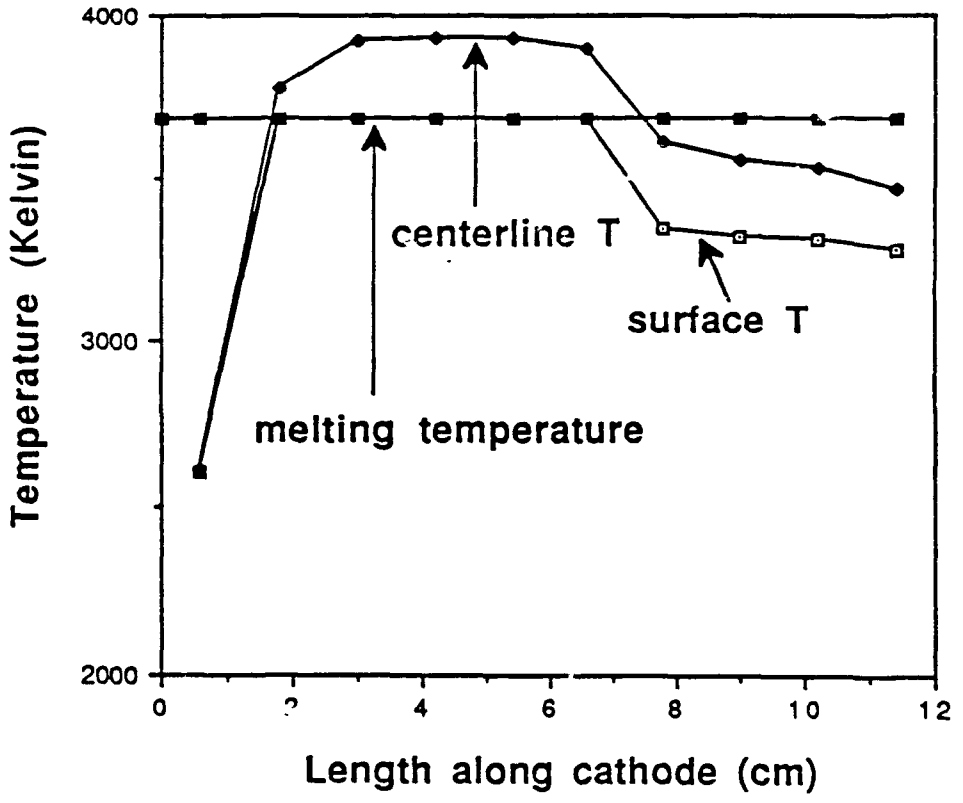

Fig.2:Shown here are calculated surface and centerline temperature profiles versus distance along the cathode for the Stuttgart ZT1 thruster. The horizontal line at 3680 K denotes the melting temperature of tungsten. Temperatures above this value cannot be taken seriously from the theoretical predictions, since the theory does not account for phenomena once melting has occurred. However, as the model suggests and as shown in this figure, the centerline temperature has exceeded the surface temperature in the select region thereby explaining the exloded cathode observed in the Stuttgart test.

Appendix

Limits on Steady Diffuse Mode Operation of the Cathode in an MPD Thruster

K. S. Hoyer,*
V. V. Subramaniam,†
Department of Mechanical Engineering
The Ohio State University
Columbus, OH 43210
and
J. L. Lawless‡
Space Power Inc.
San Jose, CA 95134

Abstract

Electrode erosion in MPD thrusters is significantly dependent on whether the mode of operation is diffuse (i.e. the net current density is distributed over the electrode surface) or via spots. Since spot mode erosion rates are typically much higher than the difuse mode erosion rates, the latter is more desirable from the standpoint of sustained steady state operation. In this paper, the steady state thermal response of the cathode in an MPD thruster is analyzed in order to determine the limits of diffuse mode operation. An energy balance at the cathode surface along with current conservation, serve to simultaneously determine the surface temperature and the total sheath voltage drop at a given location on the electrode. It is found that two different limits to steady state diffuse mode operation exist. One limit corresponds to an unsteady thermal runaway caused by excessive *electron bombardment*, in which regenerative heating leads to local melting of the electrode surface. The other limit corresponds to an operating regime where a steady state cannot exist because of increased ion bombardment. In this regime, a small increase in the net plasma current density results in a large sheath voltage drop. This causes an increase in local surface heating through ion bombardment, until a new state is reached which is inherently unsteady and accompanied by plasma oscillations. These two limits found here may correspond

---

* Graduate Student.

† DuPont Assistant Professor, Member AIAA.

‡ Senior Scientist and Manager of Advanced Concepts, Member AIAA.

to transitions from diffuse to pre-spot modes of electrode operation. These operating limits are also found to be strongly influenced by electrode and discharge parameters, as well as by external cooling.

Nomenclature

A	Thermionic emission constant
E	Electric field
e	Electronic charge
h	Heat transfer coefficient roughly representing overall heat transfer to an external coolant which is at a temperature T_{cool}
k	Boltzmann's constant
L	Cathode length
Q	Net heat per unit area per unit time into the cathode surface, at a given axial location
T	Local cathode surface temperature
V	Voltage or potential
y	Coordinate in the direction normal to the cathode surface
ε_i	Ionization potential of the propellant gas
ϕ	Electrode work function
C_e	Absolute velocity of an electron
C_{ey}	Component of the absolute velocity of an electron in the y-direction, i.e. in the direction normal to the surface
E_c	Magnitude of the y-component of the electric field at the cathode surface
E_w	y-component of the electric field at the sheath-edge
f_e	Electron velocity distribution function
j_e	Current density of plasma electrons
j_E	Surface electron emission current density

j_i Current density of plasma ions

j_∞ Net plasma current density at a given axial location

K_t Thermal conductivity of cathode material

m_e Mass of an electron

m_i Mass of an ion

n_e Electron number density

n_i Ion number density

n_∞ Charged particle number density at the edge of the collisionless sheath, at a given axial location

T_{cool} Temperature of an external coolant

T_∞ Plasma electron temperature at a given axial location

V_c Value of the voltage at the cathode surface at a given axial location, or the total voltage drop across the sheath

1. Introduction

Electrode erosion is of primary importance for the prediction of lifetimes of magnetoplasmadynamic (MPD) thrusters. Erosion processes depend on a complex coupling between plasma discharge characteristics, plasma-wall interactions, and electrode phenomena. In particular, erosion rates depend on whether the current conduction is through spots, or via a diffuse (distributed) mode. The diffuse mode is characterized by distributed current emission over the electrode surface, surface temperatures well below the material's melting temperature, and non-negligible plasma ion current. By contrast, spots are characterized by locally constricted or filamentary current conduction, surface temperatures at or above the material's melting temperature, and strong temperature-field emission. Spots are detrimental to the electrode material because of their high erosion rates[1]. Therefore, it is important to understand how and under what conditions they may be formed, and exactly when diffuse mode behaviour ends. Current understanding of this transition from diffuse to spot behaviour is at best, rather poor. In this paper, the steady state diffuse mode at the cathode is examined theoretically. Limits on thruster operation in this mode are found, and an explanation for a possible transition to spot formation is given. Additionally, the analysis yields a means of estimating cathode surface temperature which can be used to predict evaporative erosion rates for the cathode.

Earlier research on cathode processes has focused mainly on spot behaviour and spot characteristics[2-10]. Although these works reveal the intricate and complex phenomena occuring in a cathode spot, little or no information is provided as to how spots are formed in the first place. Some authors have attempted to describe transition from diffuse to spot modes. Moizhes and Rybakov[11] have found a negative-slope region in the emission current voltage characteristic, which they attribute to transition to a spot mode. These authors attribute the transition to a thermal instability, whose physical meaning or origin is totally unclear. A thermal runaway mechanism in spots due to a positive feedback between Joule heating and a temperature dependent electrical conductivity, has been proposed by Hantzsche[12]. In the same paper however, the author shows that thermionic emission cools the surface and prevents this thermal runaway. It is important to note that Hantzsche assumes the sheath voltage drop to be constant and given.

By contrast to the cathode, transition at the anode appears to have been studied more extensively[13-19]. These works attribute spot formation to an initial local surface meltdown arising primarily from Joule heating at high current densities. However, another thermal runaway mechanism involving the much ignored sheath exists[20]. In this theory, electron emission from the electrode surface decreases the sheath potential drop resulting in increased electron bombardment from the plasma. This results in a positive feedback between increased emission and heating due to electron bombardment, causing a thermal runaway. This may occur when the anode sheath voltage difference (defined here as anode potential minus the adjacent plasma potential) is negative and increasing. This thermal runaway mechanism arises before the well known anode sheath reversal[21], and may explain formation of anode spots. In this paper, the same mechanism is shown to be also operative at the cathode.

A simple model of the cathode surface and its adjacent sheath is discussed in section 2. Results for a purely thermionically emitting cathode under a range of conditions corresponding to MPD thruster operation, are given in section 3. The physical meanings of the limits on steady state diffuse mode operation are discussed in section 4, and the effects of field-enhanced and temperature-field emission are discussed in section 5. Finally, a summary of this work along with its conclusions are presented in section 6.

2. A Simple Model

This section will focus on a thermal model of the cathode surface at steady state. The cathode surface is subjected to both heating and cooling (Fig. 1). Charged particles (i.e. electrons and ions) from the plasma bombard the surface and consequently heat it. The ions (which we will assume to be singly charged) also recombine with electrons at the electrode, thereby heating the surface even further. Additional heating due to radiation from the plasma is also present and expected to be important[22], but will be neglected here. The electrode may also emit electrons which can result in heating (during field emission) or in cooling (during thermionic emission). During steady state operation, it is likely that the electrode is cooled externally[1,23]. This is usually done by cooling the cathode at its base. Finally, the cathode surface may radiate away its heat. With these considerations, we may proceed to write the following for the net heat per unit area and per unit time entering the cathode surface:

$$Q = j_e \left[\phi + \frac{2kT_\infty}{e} \right] + j_i (V_c + \varepsilon_i - \phi) - j_E \left[\phi + \frac{2kT}{e} \right] - h(T - T_{cool}) \qquad (1)$$

where Q is the net heat entering the surface per unit area and per unit time, j_e is the electron current density from the plasma into the cathode, j_i is the ion current density from the plasma into the cathode, j_E is the current density of emitted electrons from the surface, e is the charge of an electron, ϕ is the electrode work function, T_∞ is the temperature of the plasma electrons at the edge of the sheath, T is the surface temperature, V_c is the total voltage drop across the sheath, ε_i is the ionization potential of the gas (propellant), h is an overall heat transfer coefficient, and T_{cool} is the temperature of an external coolant. The quantity $h(T-T_{cool})$ represents a very rough model of the overall cooling. h can be considered as equivalent to the electrode material thermal conductivity per unit length (i.e. K_t/L). At steady state, Q must be 0 and equation (1) determines the surface temperature T. Radiative heat transfer to the anode can be shown to be negligible, and is therefore ignored here.

Consider next, the sheath region immediately adjacent to the electrode surface. This region is typically of the order of tens of Debye lengths. The electron mean free path however, is orders of magnitude larger[22]. Consequently, the sheath may be treated as a collisionless sheath. The electrons entering the sheath from the plasma are then described by the collisionless steady Boltzmann equation, which in one-dimension is:

$$C_{ey} \frac{\partial f_e}{\partial y} + \frac{eE}{m_e} \frac{\partial f_e}{\partial C_{ey}} = 0 \qquad (2)$$

where f_e is the electron velocity distribution function, C_{ey} is the component of the absolute velocity of the electrons in the direction transverse to the electrode, y is the transverse coordinate, m_e is the mass of an electron, and E is the electric field. Using the following transformations,

$$\xi = \frac{m_e C_e^2}{2kT_\infty} + \frac{eV}{kT_\infty}; \quad \text{and} \quad \eta = y \tag{3}$$

along with $E = -\partial V/\partial y$, yields:

$$\frac{\partial f_e}{\partial \eta} = 0 \quad , \; or \; that \quad f_e = f_e(\xi) \quad only \tag{4}$$

With the condition that the electron distribution function be Maxwellian at the sheath-edge (where V is taken to be 0), we obtain the following exact solution for the electron distribution function in the sheath:

$$f_e = n_e (m_e/2\pi kT_\infty)^{1/2} \exp[-m_e C_e^2/2kT_\infty] \tag{5}$$

where

$$n_e = n_\infty \exp[-eV/kT_\infty] \tag{6}$$

with n_∞ being the electron number density at the edge of the sheath where V is taken to be 0. The average flux of electrons may then be easily calculated from equations (5) and (6) by integrating f_e over dC_{ex} and dC_{ez} from $-\infty$ to ∞, and over dC_{ey} from 0 to ∞. This flux when evaluated at the wall and multiplied by e, gives the electron current density at the wall:

$$j_e = en_\infty (kT_\infty/2m_e\pi)^{1/2} \exp[-eV_c/kT_\infty] \tag{7}$$

where $-V_c$ is the potential of the cathode with respect to the sheath edge (where $V = 0$), and j_e is taken to be positive in the direction away from the cathode.

The ions entering the sheath are assumed to be monoenergetic. The Bohm criterion for a stable monotonic sheath is therefore satisfied[24]. This condition is only slightly altered in the presence of electron emission from the surface[25]. More exact theories that provide the velocity distribution function of the ions entering the sheath from the collisional pre-sheath exist[26-28]. However, for present purposes the frequently employed monoenergetic assumption simplifies the problem a great deal. We may then write the ion current density at the surface as:

$$j_i = en_\infty (k\Gamma_\infty/m_i)^{1/2} \tag{8}$$

where j_i is taken to be positive toward the cathode, m_i is the mass of the ions, and quasi-neutrality ($n_i \simeq n_e = n_\infty$) is assumed at the sheath edge. The sheath edge is a rather arbitrary definition since no such rigid demarcation exists in reality. When the ions are monoenergetic, the sheath edge has a clear meaning. However, even when the ion distribution function is not monoenergetic, the sheath edge can be defined as the location where the velocity of the ions reaches the value of the Bohm velocity $(kT_\infty/m_i)^{1/2}$. In this paper, we will adopt this definition and take the datum for the sheath potential at this location (i.e. $V = 0$ at the sheath edge). Now, If the surface emission current density denoted by j_E is taken to be positive toward the surface and

the net plasma current density denoted by j_∞ is taken to be positive toward the cathode, we may write overall current conservation at steady state as:

$$j_\infty = j_E + j_i - j_e \tag{9}$$

where in general, j_E is a function of the local surface temperature T and the local electric field at the cathode surface E_c. Determination of E_c is discussed in section 5. Equation (9) determines the total cathode sheath voltage drop V_c. Given the parameters n_∞, j_∞, T_∞, ϕ, h, T_{cool}, and the surface electric field E_c, equations (1) and (9) represent two simultaneous equations in the two unknowns, T and V_c. It must be pointed out that Crawford and Cannara mention overall current conservation in their work[29]. However their regime of interest was at very low densities (10^{14} m^{-3}), and hence ion and electron currents from the plasma were negligible in comparison with the emission current. This is an important difference between their work and the present work.

A simple solution may be found for the case of pure thermionic emission (which is likely for refractory materials), where the surface emission current density depends only on T. For this case, the total sheath voltage drop may be explicitly obtained from equation (9):

$$V_c = -\frac{kT_\infty}{e} \ln \left[\frac{j_i + j_E - j_\infty}{j_r} \right] \tag{10}$$

where $j_r = en_\infty(kT_\infty/2\pi m_e)^{1/2}$. Substituting (10) in (1) yields the following:

$$Q = \frac{2k\ j_E}{e}(T_\infty - T) + j_i\ (V_c + \varepsilon_i + \frac{2kT_\infty}{e}) - j_\infty\ (\phi + \frac{2kT_\infty}{e}) - h\ (T - T_{cool}) \tag{11}$$

Since at steady state Q must be zero, equation (11) represents an implicit equation for the local surface temperature T, where V_c is given by (10).

An interesting phenomenon is revealed by equation (11). The emission current density which under thermionic conditions results in energy transport away from the cathode, appears as an input heating source. This can be understood upon close examination of equation (9) or (10). When the emission current density increases for a fixed plasma number density and plasma current density, the sheath voltage drop must decrease in order to conserve total current. This results in an increase in electron bombardment, which contributes to heating the surface. Thus, although thermionic emission cools the surface, its overall effect is to *heat* the surface via increased electron bombardment. It is therefore important to include the effects of the sheath when attempting to determine the surface temperature.

A simple model has been developed in this section, which considers a thermal balance of the cathode surface along with overall current conservation. The local surface temperature and overall sheath voltage drop can be determined from this. Results for a purely thermionically emitting cathode under typical MPD conditions are presented

next.

3. Results for Pure Thermionic Emission

The governing equations presented in the preceding section are solved in this section for the case of pure thermionic emission (i.e. no field enhanced or temperature-field emission). Temperatures and sheath voltage drops are calculated for typical MPD conditions.

For pure thermionic emission, the emission current density is given by:

$$j_E = AT^2 exp[-e\phi/kT] \tag{12}$$

where A is the emission coefficient and ϕ is the material work function. The sheath voltage drop V_c can then be written in terms of T using equation (10). Given the parameters n_∞, j_∞, T_∞, ϕ, h, and T_{cool}, equations (10), (11) and (12) may be combined and solved for T. The sheath voltage drop can then be determined from (10). The emission coefficient may vary considerably for materials with oxide layers. Both A and ϕ may vary locally on a given surface, so that it is important to consider the sensitivity of final results to variations in these parameters. This is addressed later in this section.

A typical variation of the net heat into the cathode (Q) versus the surface temperature, is displayed in Fig. 2. Two intersections with the horizontal axis are found, representing two possible steady state solutions. The first (lower temperature) is a stable attractor, while the second (higher temperature) is an unstable repeller. This can be seen quite easily by perturbing the solutions to either side, and determining if the initial state is restored. The physical meaning of the stable point is clear. The incoming energy on the surface is exactly balanced by the outgoing energy. Furthermore, the surface can maintain this temperature for an indefinite period of time even for small fluctuations in the discharge. The unstable point requires some explanation. Although an exact balance between incoming and outgoing energy is possible at this point, the surface cannot remain in this state indefinitely and is susceptible to change due to infinitesimal fluctuations. Physically, this state represents an operating regime where the temperature and hence the emission current density is high enough to lower the sheath voltage drop below a critical value. This causes excessive heating due to increased electron bombardment, resulting in a temperature rise. The subsequent increase in temperature causes an increase in current emission which lowers the sheath voltage drop further. This positive feedback process then repeats itself until the surface is regeneratively heated upto the melting temperature. This effect is quantitatively described in section 4.

Results from the present calculation are shown in Figs. 3-6. In these figures, the steady state surface temperatures calculated from equation (11) are shown versus the net plasma current density j_∞, the charged particle number density at the sheath edge n_∞, the electrode work function ϕ, and the temperature of the external coolant T_{cool}. The heat transfer coefficient h is fixed at 20 kW/m^2/K, the plasma electron temperature is taken to be 12000 K, and $A = 3 \times 10^4$ $A/m^2/K^2$. The value of h is

obtained from an estimate of the thermal conductance through a tungsten cathode. All four plots display both the stable (lower temperature) and unstable (higher temperature) regimes. Figures 3 and 4 display the variation of T with j_∞ and n_∞ respectively for $\phi = 2.63$ V and $T_{cool} = 500$ K. From Fig. 3, it can be seen that for a given number density, the stable diffuse mode is limited both at low as well as high values of the current density. Similarly, for a given current density there are lower and upper limits on the range of allowable number densities. At low current densities (n_∞ fixed) and at high number densities (j_∞ fixed), the stable and unstable solutions are seen to merge and disappear. Also, at the higher current densities (n_∞ fixed) and the lower number densities (j_∞ fixed), the stable diffuse operation is limited and only the unstable mode exists. It is interesting to note that for a given number density, the steady state, stable surface temperature does not vary significantly with the current density over a wide range (see Fig. 3). This is because in this region, the ion current primarily determines the sheath voltage drop which is then to a very good approximation a constant since the number density is fixed. Heating due to ion bombardment is then balanced by the external cooling. Therefore, inspection of equation (11) reveals that the surface temperature should not depend significantly on j_∞ in this region. By contrast, changes in n_∞ at a fixed j_∞ affect the stable operation drastically via increased electron and/or ion bombardment. This is reflected in Fig. 4. The variation of the surface temperatures with electrode work function is shown in Fig. 5 for $T_{cool} = 500$ K, $j_\infty = 10^6$ A/m^2, and $n_\infty = 8 \times 10^{21}$ m^{-3}. The previously discussed stable and unstable regimes are again found to exist. The stable, steady state surface temperature is almost invariant with respect to ϕ in this regime, again because the ion current principally determines the sheath drop, and ion bombardment dominates. Also shown in this figure is the solution for a different value of the thermionic emission constant ($A = 120 \times 10^4$ $A/m^2/K^2$). The effect of a higher value of A is simply to shift the turning point (i.e. the point where stable and unstable solutions merge and then disappear) toward the higher work function side. Otherwise, the stable, steady state surface temperature is practically the same as for a lower value of A, since ion bombardment is still the dominant mechanism. Figure 6 displays the surface temperatures versus the external coolant temperature for $\phi = 2.63$ V, $j_\infty = 10^6$ A/m^2, $n_\infty = 5 \times 10^{21}$ m^{-3}, and $h = 20$ $kW/m^2/K$. Both stable and unstable regimes are seen to exist, and exhibit the features that have just been discussed.

This section has focused on results for a thermionically emitting cathode operating under typical MPD conditions. Stable and unstable regimes as well as limits on steady state operation have been found. These limits are found to be strongly influenced by both discharge and electrode parameters. The next section will focus on a detailed discussion of the operating limits that have been found.

4. Limits on the Steady Diffuse Mode

In this section, two different mechanisms that lead to local melting of the cathode surface are discussed. The first mechanism is an excessive heating due to electron bombardment, that occurs when the sheath voltage drop falls below a critical value. A

positive feedback between electron bombardment and surface electron emission results in this thermal runaway. The second mechanism is heating due to ion bombardment, which dominates as the sheath voltage drop increases sharply for a relatively small increase in the plasma current density. A steady state can no longer be maintained, unless plasma discharge parameters change dramatically.

We consider the thermal runaway mechanism first. The value of the critical voltage drop at which the thermal runaway due to electron bombardment occurs, can be obtained quite readily for the case of pure thermionic emission. For a given plasma current density and plasma number density at the sheath edge, equation (10) may be substituted into equation (11) and the resulting expression differentiated with respect to T to yield:

$$\frac{\partial Q}{\partial T} = -h + \frac{2kj_E}{e}\left[-\frac{e\phi}{kT} - 3\right] + \frac{2kT_\infty j_E}{eT}\left[2 + \frac{e\phi}{kT}\right]\left[1 - \frac{j_i}{2j_e}\right] \qquad (13)$$

For stability (in the Lyapunov sense), we require that $\partial Q/\partial T$ be less than zero. A *sufficient* condition for stability from (13) is:

$$\frac{j_i}{j_e} \geq 2 \qquad (14)$$

which by using (7) and (8), gives a condition on the sheath voltage drop V_c:

$$V_c \geq \frac{kT_\infty}{2e} \ln\left[\frac{2m_i}{\pi m_e}\right] \qquad (15)$$

For argon and an electron temperature of 12000 K, this yields an approximate value of 5.5 V for the critical sheath voltage drop. It is important to note that this is only a *sufficient* condition for stability. From equation (13), it can be seen that the exact value of the critical voltage drop depends on the electrode properties (work function and emission current), surface temperature, and external cooling (h). This more general criterion on the total sheath voltage drop necessary to ensure stability of a given steady state is:

$$V_c \geq \frac{kT_\infty}{2e} \ln\left[\left(\frac{m_i}{2\pi m_e}\right)^{1/2}\left(2 - \frac{T(3+e\phi/kT)}{T_\infty(2+e\phi/kT)} - \frac{ehT}{kj_E T_\infty(2+e\phi/kT)}\right)\right] \qquad (16)$$

Above the value given by the critical voltage drop, a steady state defined by (10) and (11) (with $Q = 0$) can be maintained indefinitely even for small fluctuations in n_∞ and j_∞. Below this value, the positive feedback between electron bombardment and surface electron emission leads to thermal runaway and a stable steady state cannot be maintained. The surface subsequently melts locally. Alternatively, the condition $\partial Q/\partial T < 0$ may be interpreted as providing a constraint on the amount of cooling (i.e the value of h) necessary for steady and stable operation. Equation (14) along with (9) may therefore be rewritten in the following form, yielding an important upper limit on the local surface temperature for diffuse operation:

$$j_E(T) = AT^2 exp(-e\phi/kT) \leq j_\infty - j_e \qquad (17)$$

Under MPD conditions, the critical temperatures predicted by equation (17) are well

below the material melting temperature.

A second mechanism exists that can cause local melting of the cathode surface. For high j_∞ (given an n_∞) or low n_∞ (given a j_∞), it is possible that $j_\infty \rightarrow j_i + j_E$. When this occurs, the total sheath voltage drop increases sharply. This can be seen from equation (10) where $V_c \rightarrow \infty$ as $j_\infty \rightarrow j_i + j_E$. This has two important consequences. First, emitted electrons cause increased ionization outside the sheath since they gain large amounts of energy after traversing the sheath. Second, the ions gain substantial amounts of energy while falling through the sheath. These cause a rapid increase in ion bombardment with subsequent heating of the surface. This temperature rise necessarily results in increased surface electron emission. Consequently, there arises a conflict between the emission current necessary for cooling the cathode surface (i.e. to balance heating by ion bombardment) and the emission current necessary to preserve overall current conservation at steady state. The increasing sheath drop also drastically reduces the electron current from the plasma necessary to counteract an increasing emission current, and hence maintain a steady state. This leads to unsteady behaviour in the sheath, thereby forcing the surface and the plasma to also become unsteady. The local surface temperature can rise due to ion bombardment in the meanwhile, until the surface has locally melted. Although the present theory becomes inapplicable at this point, it is capable of predicting this limit. An important phenomenon associated with this second mechanism but not with the first, is the triggering of plasma oscillations[30]. When the sheath voltage drop rises and approaches energies equal to or greater than that of the first excited states of the propellant atoms, ionization levels can be enhanced in the pre-sheath region. Also, while the thermionically emitted electrons relax their momenta relatively quickly due to elastic collisions with neutrals, their energy relaxation times are much longer due to infrequent collisions with plasma electrons. When the number density of thermionically emitted ("beam") electrons approaches the local number density of plasma electrons, longitudinal oscillations can result[30]. This condition may be quantitatively expressed within the context of the present work as:

$$n_e \ll 2.563x10^{13}\, j_E^{2/5}\, V_C^{8/5} \tag{18}$$

where n_e is the number density of plasma electrons immediately adjacent to the sheath. This second mechanism which is related to a high back-EMF, may explain the Onset phenomenon observed in the MPD thrusters[32,33].

The two aforementioned mechanisms responsible for limiting the diffuse mode, also cause local melting of the cathode surface. Local surface melting may be a precursor to spot formation. However, it must be pointed out that an intermediate stable state may exist where molten regions that are submicron in size (microspots[1]) are scattered over the cathode surface, while most of the discharge appears diffuse. It is therefore possible that the two mechanisms found and discussed here, correspond to transitions from diffuse to spot mode or another intermediate mode with microspots.

5. Effects of Field-Enhanced and T-F Emission

We have thus far considered a purely thermionically emitting cathode. In general however, the emission current density depends both on the surface temperature and on the surface electric field[31]. In this section, the influence of this field-enhanced (also known as Schottky emission) and temperature-field (T-F) emission is evaluated and discussed.

The governing equations for the sheath and the cathode surface are described by the surface energy balance (equation (1)) and overall current conservation (equation (9)). These equations are still applicable in the presence of an electric field at the surface of the cathode. However, a simple analytic solution cannot be obtained because the sheath voltage drop cannot be explicitly determined in terms of the surface temperature. This is because the emission current density in (9) depends on T and E_c, and E_c in turn depends on V_c. The required additional equation for E_c may be obtained from a solution of Poisson's equation in the sheath. An outline of this procedure is given by Prewett and Allen[25] for the case of a constant surface emission current density. Extension of their solution for the potential distribution in the sheath for the case where the emission current density depends on both T and E_c, is straightforward and will not be discussed here. The additional equation for E_c for monoenergetic ions is the following implicit equation:

$$\frac{\varepsilon_o}{2}\left(E_c^2 - E_w^2\right) \approx n_\infty kT_\infty \left[\left[1 + \frac{2eV_c}{kT_\infty} \right]^{1/2} - 2 + exp\left[-eV_c/kT_\infty\right] \right] - j_E (2m_e V_c/e)^{1/2} \qquad (19)$$

where E_w is the electric field at the sheath edge where $V = 0$. In general, E_w is much smaller than E_c and may be ignored. j_E is the emission current density which may be calculated from quantum-mechanical considerations. A general integral expression for j_E as a function of T and E_c is given by Murphy and Good[31]. For low values of E_c, j_E may be simply expressed by the well known Schottky formula[31]. For the higher values of E_c, the emission is influenced by both E_c and T, and is known as T-F emission. Thus, equations (1) with $Q = 0$, (9), and (17) represent three coupled and non-linear equations for the three unknowns T, V_c, and E_c. This system has been solved numerically. It is also possible to numerically integrate Poisson's equation to determine the variation of the potential and the electric field in the sheath. Figure 7 displays the computed variation of the electric field versus vertical distance from the surface for a particular value of j_∞ and n_∞. However, it must be pointed out that the resulting profiles represent the solution within the sheath only. A uniformly valid solution for the sheath, transition region, and the plasma beyond has to be obtained through matched asymptotic expansions[26,27,28]. Consequently, the solution of Poisson's equation given here represents only the "inner" solution. For the range of parameters considered in this paper, computed values of E_c are of the order of 10^7 V/m or less. Such values of the electric field produce a negligible increase in current emission at surface temperatures of interest to the MPD thruster. Consequently, the stable diffuse mode is well represented by pure thermionic emission

6. Discussion and Conclusions

The thermal response of the cathode in an MPD thruster has been studied under steady state diffuse conditions. The electrode-adjacent sheath has been included for monoenergetic ions. The solution of Poisson's equation in the sheath together with overall current conservation and an energy balance at the electrode surface, serve to determine the electric field at the surface, the surface temperature, and the total sheath voltage drop simultaneously and self-consistently. Two operating regimes are found. One is stable, while the other is an unstable thermal runaway caused by excessive *electron bombardment*. The thermal runaway leads to eventual local melting of the cathode surface, and may be a precursor to spot formation. The stable steady state on the other hand, is strongly influenced by discharge and electrode parameters. The values of n_∞, j_∞, and T_∞ used here have been obtained from an approximate non-equilibrium model of the electrode-adjacent flow[22]. The rate of cooling is found also to be extremely important. Varying values of h result in two operating regimes, similar to the results displayed in Fig. 6. Furthermore, the dependence of the surface temperature on h is quite significant. For $n_\infty = 5 \times 10^{21}$ m^{-3}, $j_\infty = 10^6$ A/m^2, T_{cool} = 500 K, and ϕ = 2.63 V, a 1% decrease in h results in about a 10% increase in the local surface temperature (see Fig. 8). Of course for h larger ($\simeq 10^5$ $W/m^2/K$) than the value used here, the variation is less dramatic but still non-negligible.

Two mechanisms are found to be responsible for destabilizing the stable, steady, diffuse mode. The first occurs at values of the sheath voltage drop *below* a critical value. Small sheath voltage drops lead to increased electron bombardment and subsequent thermal runaway if the cooling is insufficient. Such a condition can occur in the MPD thruster operating at near-onset total currents. Near onset, the current density is sharply peaked and large near the inlet and the exit regions, while going through a minimum in the middle region (in the axial direction) of the thruster. The current density in the middle region of the thruster becomes smaller with increasing total current to the thruster, due to a high back-EMF[32,33] which then leads to smaller sheath voltage drops. The second mechanism due to excessive ion bombardment and accompanied by plasma oscillations, occurs at high values of the current density (for a given plasma number density) or for low values of the plasma number density (for a given current density). Here, high sheath voltage drops result in increased ion bombardment leading to increased surface electron emission. Since plasma electrons are repelled at high sheath potentials, overall current conservation given by (9) cannot be satisfied at steady state. The sheath is then no longer steady. The second mechanism may be inhibited if an increase in the sheath-edge charged particle number density n_∞ occurs via increased ionization due to electrons emitted from the cathode surface. Clearly, this requires overall sheath voltage drops of the order of the propellant ionization potential. The occurence of both mechanisms is strongly influenced by discharge parameters.

The simple model discussed in this paper represents a first attempt at relating the plasma discharge, the sheath, and the electrode. Although this model has revealed some important underlying physics, there are several deficiencies. First, the pre-sheath has not been considered in detail. The pre-sheath is important not only for determining the ion velocity distribution function, but also for asymptotically

determining a uniformly valid potential distribution. This potential distribution will then yield the correct variation in the sheath when considered on the scale of the Debye length, and will also yield the correct variation in the plasma when viewed on the macroscopic length scale in the problem. Such pre-sheath solutions exist as mentioned previously in section 2, but only for charge-exchange reactions or in the absence of surface electron emission. For the plasma in the MPD thruster, additional ionization by electrons emitted from the surface is important under some conditions. Second, radiative heating of the electrode surface by the plasma has been neglected. This not only contributes to direct heating, but also to increased heating by particle bombardment via increased charged particle number densities at the sheath-edge. Radiative transfer in the MPD plasma is a topic for detailed study. Although these two deficiencies can affect the quantitative predictions of the surface temperature, they will not affect the existence of the thermal runaway mechanism and unstable operating regimes found here. The theory presented in this paper together with models of the flowing plasma[22,32,33], provide the designer with a number of tools. In addition to the prediction of erosion rates under a variety of possible operating conditions, the proper cathode length, diameter, material, external cooling conditions, and choice of propellant can be systematically evaluated.

Experimental verification of the predictions of the theory presented in this paper requires simultaneous measurement of the plasma current density, plasma charged particle number density near the electrode, amount of external cooling, and the local surface temperature. Although temperature measurements in low-power steady-state MPD thrusters have been made[34], lack of knowledge with regard to the local current and number densities makes comparison between this theory and existing measurements unreliable. The measured steady state cathode surface temperatures in a subscale device for thoriated tungsten, range from 2087 K to 2281 K for a range of total currents from 500 A to 1200 A and mass flows from 46.4 mg/s to 150.8 mg/s[34]. This is comparable to the parameter range considered in this paper. Despite the difficulties encountered in non-intrusively measuring plasma number densities and current densities, efforts to measure these variables along with the local surface temperature would be desirable and invaluable. Such local surface temperature measurements if based on optical pyrometry, must also account for reflection from the radiating MPD plasma. As a final point, it must be mentioned that scanning electon micrographs (SEMs) of used cathodes *always* display evidences of craters from spots and microspots in some regions. These spots can easily be formed during the start-up transient or the shut-down transient of the arc. Therefore, future experiments aimed at understanding the diffuse mode limits must exercise great caution to make sure that spots are not formed during arc initiation or shut-down.

Acknowledgements

This work was supported by the Air Force Office of Scientific Research grant no. AFOSR-87-0360, and in part by a DuPont Young Faculty Award.

References

(1) Schrade, H. O., Auweter-Kurtz, M., and Kurtz, H. L., "Cathode Erosion Studies on MPD Thrusters", *AIAA Journal*, Vol. 25, No. 8, August 1987, pp. 1105-1112.

(2) Ecker, G., "The Vacuum Arc Cathode - A Phenomenon Of Many Aspects", *IEEE Trans. Plasma Sci.*, Vol. PS-4, No. 4, December 1976, pp. 218-227.

(3) Harstad, K., "Electrode Processes in MPD Thrusters", JPL Publication 81-114, March 1982.

(4) Guile, A. E., and Juttner, B., "Basic Erosion Processes of Oxidized and Clean Metal Cathodes by Electric Arcs", *IEEE Trans. Plasma Sci.*, Vol. PS-8, No. 3, September 1980, pp. 259-269.

(5) Schrade, H. O., Auweter-Kurtz, M., Kurtz, H. L., "Analysis of the Cathode Spot of Metal Vapor Arcs", *IEEE Trans. Plasma Sci.*, Vol. PS-11, No. 3, September 1983, pp. 103-110.

(6) Guile, A. E., and Hitchcock, A. H., "Oxide films on arc cathodes and their emission and erosion", *J. Phys. D: Appl. Phys.*, Vol. 8, 1975, pp. 663-669.

(7) Cheng, D. Y., "Dynamics of Arc Ignition and Cathode Spot Movement of Thermionically Emitting Cathode Surfaces", *J. Appl. Phys.*, Vol. 41, No. 9, August 1970, pp. 3626-3633.

(8) Rakhovsky, V. I., "Current Density per Cathode Spot in Vacuum Arcs", *IEEE Trans. Plasma Sci.*, Vol. PS-12, No. 3, September 1984, pp. 199-203.

(9) Prock, J., "Time-Dependent Description of Cathode Crater Formation in Vacuum Arcs", *IEEE Trans. Plasma Sci.*, Vol. PS-14, No. 4, August 1986, pp. 482-491.

(10) Ecker, G., "Theoretical Aspects of the Vacuum Arc", in *Vacuum Arcs*, J. M. Lafferty, Ed. New York: Wiley, 1980, pp. 228-320.

(11) Moizhes, B. Ya., and Rybakov, A. B., "Transition from Distributed Emission to a Cathode Spot in an Arc", *Sov. Phys. Tech. Phys.*, Vol. 15, No. 9, March 1971, pp. 1574-1576.

(12) Hantzsche, E., "Thermal Runaway Prevention in Arc Spots", *IEEE Trans. Plasma Sci.*, Vol. PS-11, No. 3, September 1983, pp. 115-122.

(13) Miller, H. C., "Vacuum Arc Anode Phenomena", "*IEEE Trans. Plasma Sci.*, Vol. PS-11, No. 2, June 1983, pp. 76-89.

(14) Lafferty, J. M., "Triggered Vacuum Gaps", *Proc. IEEE*, Vol. 54, 1966, pp. 23-32.

(15) Jolly, D. C., "Anode Surface Temperature and Spot Formation Model for the

Vacuum Arc", *J. Appl. Phys.*, Vol. 53, 1982, pp. 6121-6126.

(16) Ecker, G., "Anode Spot Instability. I. The Homogeneous Short Gap Instability", *IEEE Trans. Plasma Sci.*, Vol. PS-2, 1974, pp. 130-146.

(17) Schuocker, D., "Improved model for anode spot formation in vacuum arcs", *IEEE Trans. Plasma Sci.*, Vol. PS-7, 1979, pp. 209-216.

(18) Boxman, R. L., "Magnetic constriction effects in high-current vacuum arcs prior to the release of anode vapor", *J. Appl. Phys.*, Vol. 48, 1977, pp. 2338-2345.

(19) Kimblin, C. W., "Anode Voltage Drop and Anode Spot Formation in DC Vacuum Arcs", *J. Appl. Phys.*, Vol. 40, 1969, pp. 1744-1752.

(20) Subramaniam, V. V., and Lawless, J. L., "Thermal Instabilities of the Anode in a Magnetoplasmadynamic Thruster", *AIAA J. Propulsion and Power*, Vol. 6, No. 2, March-April 1990, pp. 221-224.

(21) Hugel, H., "Effect of Self-Magnetic Forces on the Anode Mechanism of a High Current Discharge", *IEEE Trans. Plasma Sci.*, Vol. PS-8, No. 4, December 1980, pp. 437-442.

(22) Subramaniam, V. V., and Lawless, J. L., "Electrode-Adjacent Boundary Layer Flow in Magnetoplasmadynamic Thrusters", *Phys. Fluids*, Vol. 31, No. 1, January 1988, pp. 201-209.

(23) King, D. Q., private communication, June 9, 1988.

(24) Bohm, D., "Minimum Ionic Kinetic Energy for a Stable Sheath", in *Characteristics of Electrical Discharges in Magnetic Fields*, A. Guthrie and R. Wakerling, Eds. New York: McGraw-Hill, 1949, pp. 77-86.

(25) Prewett, P. D., and Allen J. E., "The Double Sheath Associated with a Hot Cathode", *Proc. R. Soc. Lond. A.* **348**, 1976, pp. 435-446.

(26) Riemann, K. -U., "Kinetic theory of the plasma sheath transition in a weakly ionized plasma", *Phys. Fluids*, Vol. 24, No. 12, December 1981, pp. 2163-2172.

(27) Emmert, G. A., Wieland, R. M., Mense, A. T., and Davidson, J. N., " Electric sheath and presheath in a collisionless, finite ion temperature plasma", *Phys. Fluids*, Vol. 23, No. 4, April 1980, pp. 803-812.

(28) Main, G., "Asymptotically correct collisional presheaths", *Phys. Fluids*, Vol. 30, No. 6, June 1987, pp. 1800-1809.

(29) Crawford, F. W., and Cannara, A. B., "Structure of the Double Sheath in a Hot Cathode Plasma", *J. Appl. Phys.*, Vol. 36, No. 10, October 1965, pp. 3135-3141.

(30) A. F. Alexandrov, L. S. Bogdankevich, and A. A. Rukhadze, *Principles of Plasma Electrodynamics*, Springer-Verlag, New York, 1984.

(31) Murphy, E. L., and Good Jr., R. H., "Thermionic Emission, Field Emission, and the Transition Region", *Physical Review*, Vol. 102, No. 6, June 15, 1956, pp. 1464-1473.

(32) Lawless, J. L., and Subramaniam, V. V., "Theory of Onset in Magnetoplasmadynamic Thrusters", *AIAA J. Propulsion and Power*, Vol. 3, No. 2, March-April 1987, pp. 121-127.

(33) Subramaniam, V. V., and Lawless, J. L., "Onset in Magnetoplasmadynamic Thrusters with Finite Rate Ionization", *AIAA J. Propulsion and Power*, Vol. 4, No. 6, November-December 1988, pp. 526-532.

(34) D. Q. King, private communication, September 7, 1988.

Figure Captions

Fig. 1: The cathode is shown here along with the various heating and cooling mechanisms.

Fig. 2: A typical variation of the net heat per unit area per unit time into the cathode surface is shown here versus surface temperature. This is the variation predicted by equations (10) and (11) in section 2.

Fig. 3: The steady state surface temperature as predicted by equations (10) and (11) is shown here versus the net plasma current density j_∞ for various values of n_∞. The other parameters are $h = 20\ kW/m^2/K$, $\phi = 2.63$ V, $T_{cool} = 500$ K, $A = 3 \times 10^4\ A/m^2/K^2$, and $T_\infty = 12000$ K.

Fig. 4: The steady state surface temperature as predicted by equations (10) and (11) is shown here versus the net plasma current density n_∞ for various values of j_∞. The other parameters are $h = 20\ kW/m^2/K$, $\phi = 2.63$ V, $T_{cool} = 500$ K, $A = 3 \times 10^4\ A/m^2/K^2$, and $T_\infty = 12000$ K.

Fig. 5: The steady state surface temperature as predicted by equations (10) and (11) is shown here versus the electrode work function ϕ for $j_\infty = 10^6\ A/m^2$, $n_\infty = 8 \times 10^{21}\ m^{-3}$, $T_{cool} = 500$ K, $h = 20\ kW/m^2/K$, and $T_\infty = 12000$ K.

Fig. 6: The steady state surface temperature as predicted by equations (10) and (11) is shown versus the external coolant temperature T_{cool} for $\phi = 2.63$ V, $j_\infty = 10^6\ A/m^2$, $h = 20\ kW/m^2/K$, $A = 3 \times 10^4\ A/m^2/K^2$, and $T_\infty = 12000$ K.

Fig. 7: The variation of the electric field (-E) in the steady, collisionless electrode-adjacent sheath is displayed here versus vertical distance from the cathode surface. This plot is a result of integrating the Poisson equation with the limits of integration provided by a simultaneous solution of equations (1) (with $Q = 0$), (9), and (17). The case displayed here is for $j_\infty = 10^6\ A/m^2$, $n_\infty = 5 \times 10^{21}\ m^{-3}$, $T_\infty = 12000$ K, $T_{cool} = 500$ K, $\phi = 2.63$ V, $h = 20\ kW/m^2/K^2$. The calculated surface temperature is 1824 K, and the value of the electric field at the cathode surface is 1.76×10^7 V/m. Note that the electric field is negative because of the convention used here. The actual field is positive, i.e. pointing toward the surface.

Fig. 8: The variation of the cathode surface temperature as predicted by equations (10) and (11) is shown here versus the heat transfer coefficient h, for a net current density of $j_\infty = 10^6\ A/m^2$, and for two different number densities. The other parameters are $T_\infty = 12000$ K, $\phi = 2.63$ V, and $T_{cool} = 500$ K.

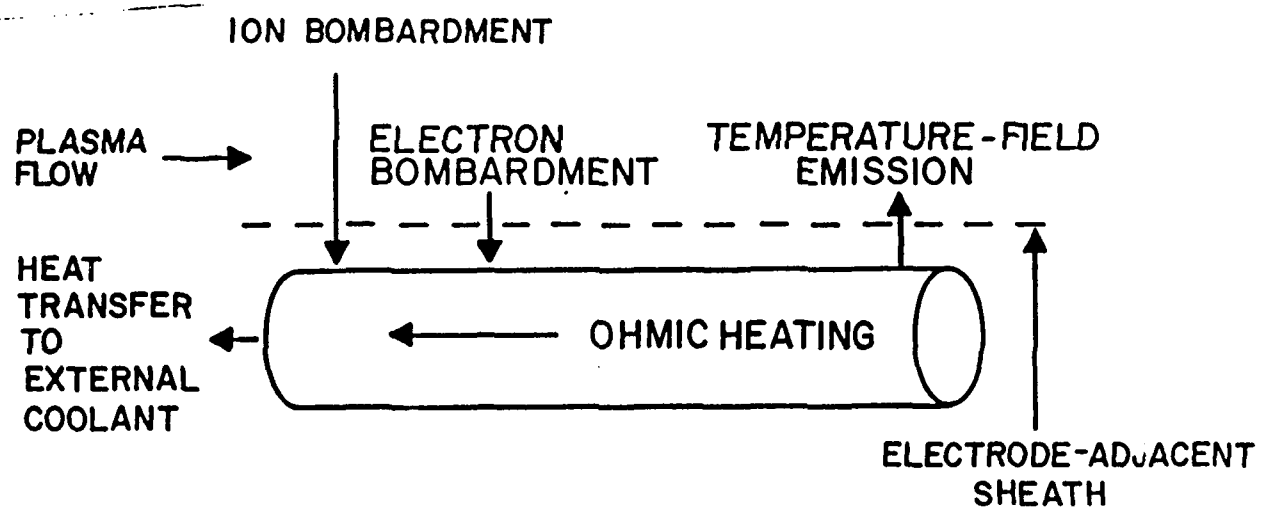
ION BOMBARDMENT
PLASMA FLOW
ELECTRON BOMBARDMENT
TEMPERATURE-FIELD EMISSION
HEAT TRANSFER TO EXTERNAL COOLANT
OHMIC HEATING
ELECTRODE-ADJACENT SHEATH

Fig. 1

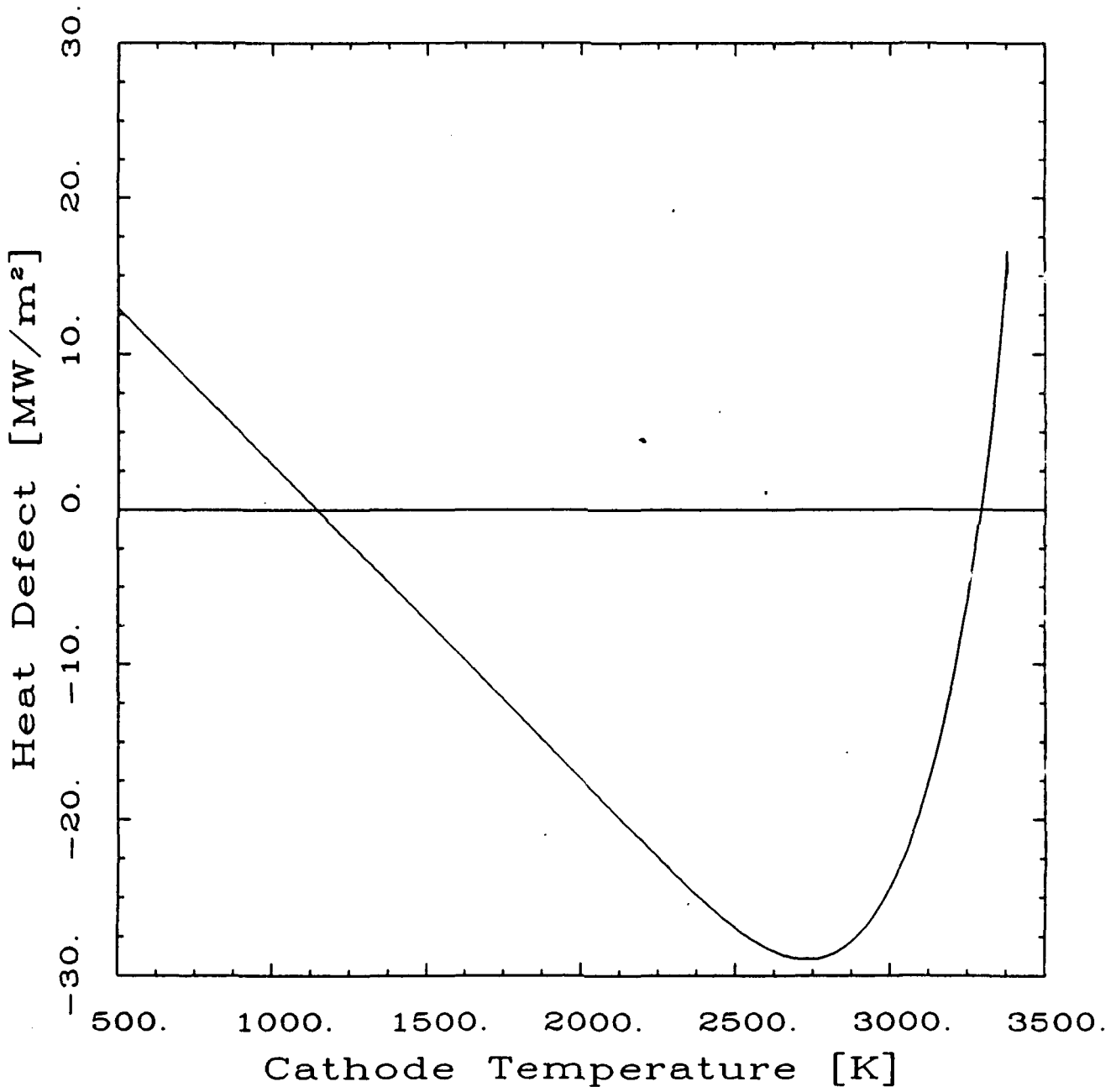
Heat Defect [MW/m²]
30.
20.
10.
0.
−10.
−20.
−30.
500.
1000.
1500.
2000.
2500.
3000.
3500.
Cathode Temperature [K]

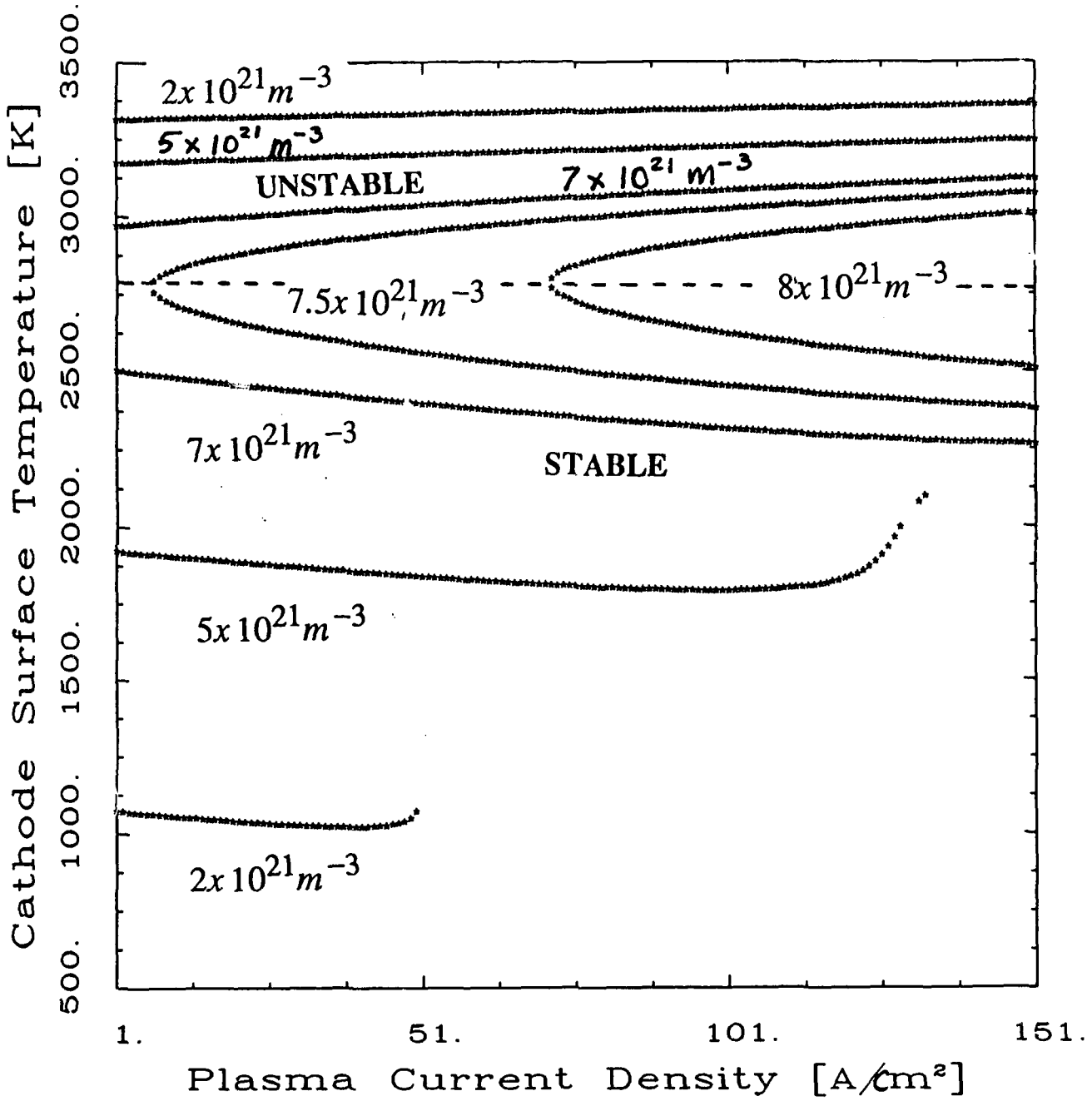
Cathode Surface Temperature [K]
500.
1000.
1500.
2000.
2500.
3000.
3500.
$2x\,10^{21}m^{-3}$
$5\times10^{21}\,m^{-3}$
UNSTABLE
$7\times10^{21}\,m^{-3}$
$7.5x\,10^{21}m^{-3}$
$8x\,10^{21}m^{-3}$
$7x\,10^{21}m^{-3}$
STABLE
$5x\,10^{21}m^{-3}$
$2x\,10^{21}m^{-3}$
1.
51.
101.
151.
Plasma Current Density [A/cm²]

Fig. 3

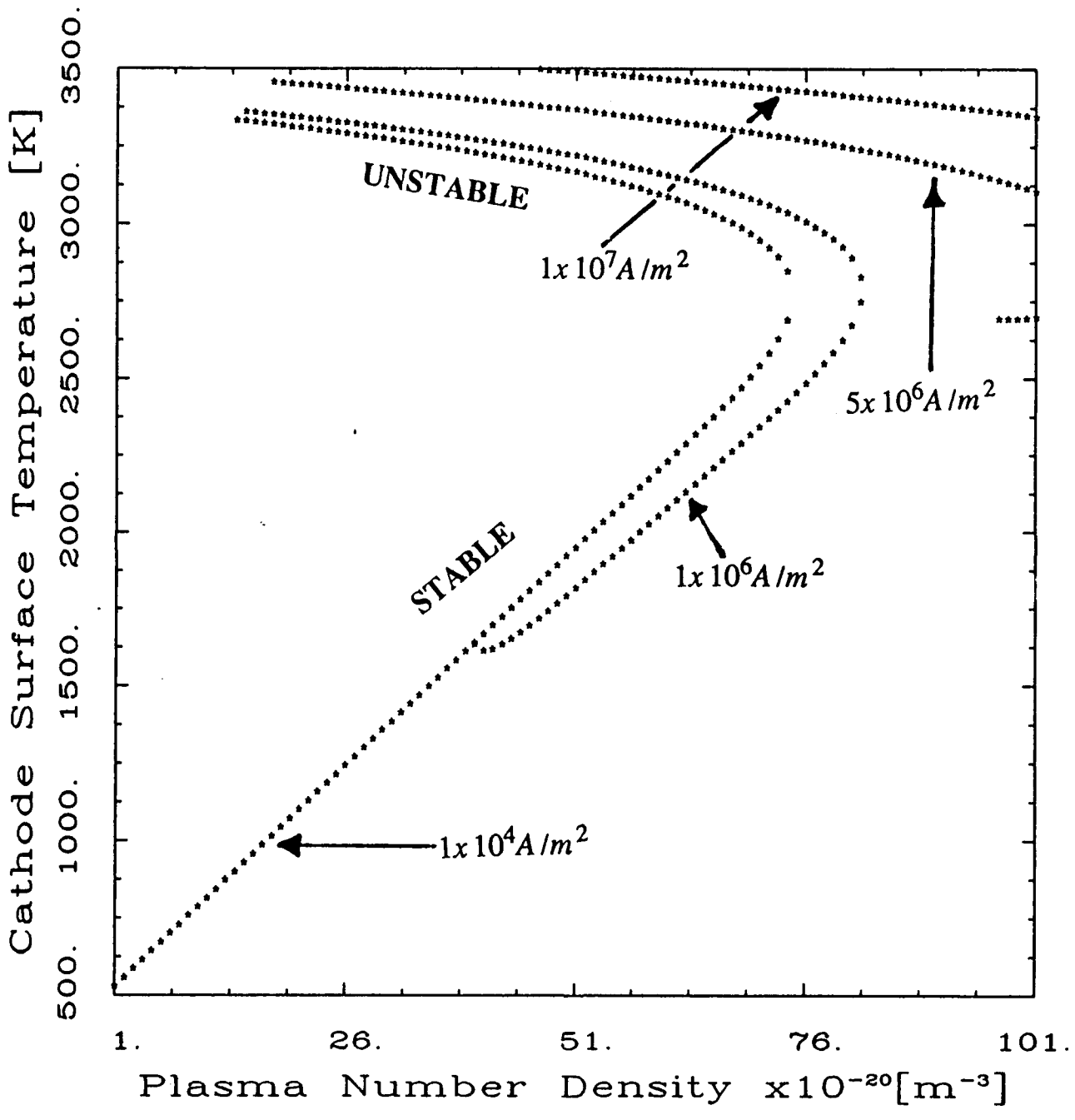
Cathode Surface Temperature [K]
500.
1000.
1500.
2000.
2500.
3000.
3500.
UNSTABLE
STABLE
1x 10^7 A/m^2
5x 10^6 A/m^2
1x 10^6 A/m^2
1x 10^4 A/m^2
1.
26.
51.
76.
101.
Plasma Number Density x10^-20[m^-3]

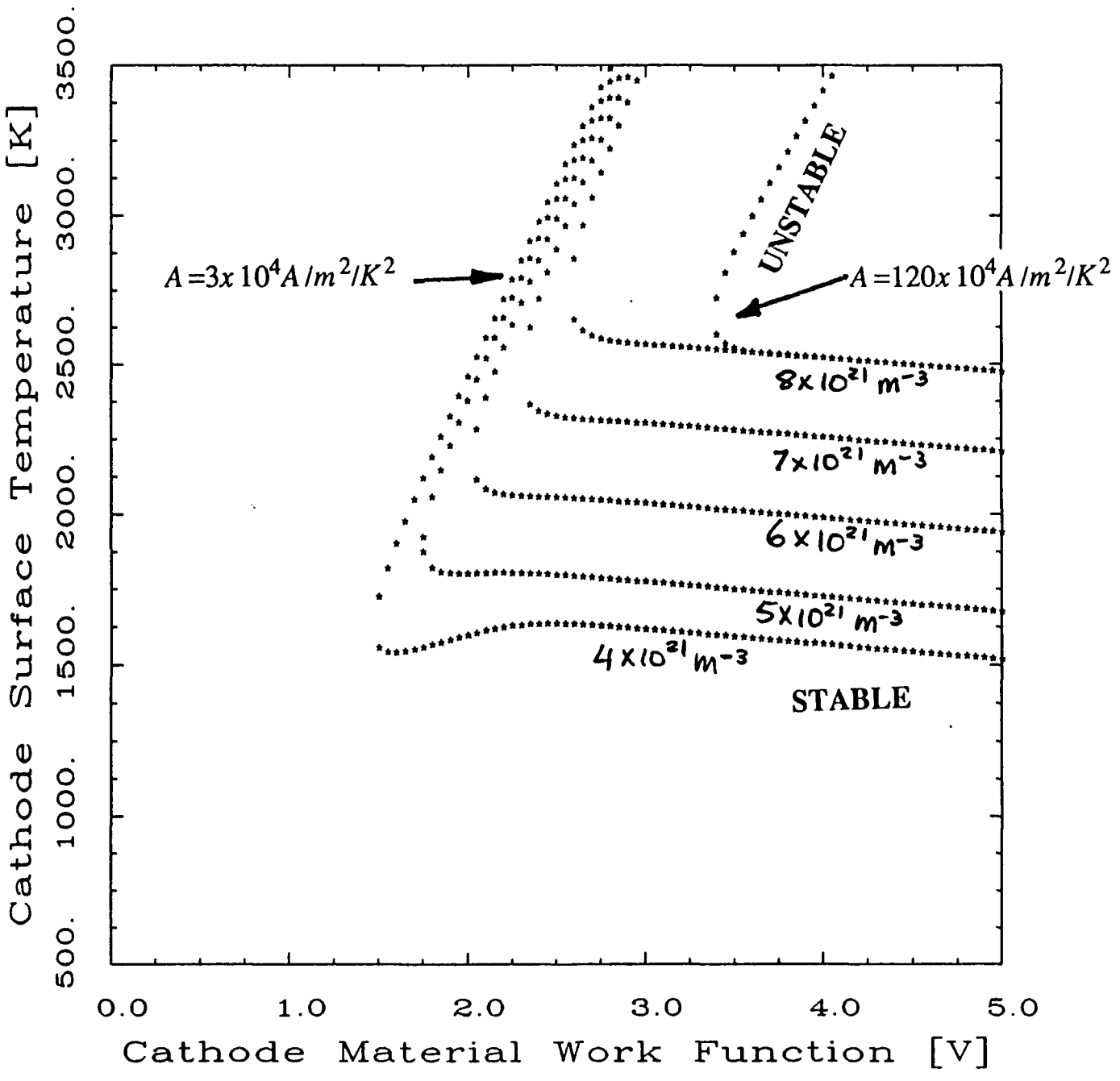
Cathode Surface Temperature [K]
500.
1000.
1500.
2000.
2500.
3000.
3500.
0.0
1.0
2.0
3.0
4.0
5.0
Cathode Material Work Function [V]
A =3x 10^4 A /m^2/K^2
A =120x 10^4 A /m^2/K^2
UNSTABLE
8x10^21 m^-3
7x10^21 m^-3
6x10^21 m^-3
5x10^21 m^-3
4x10^21 m^-3
STABLE

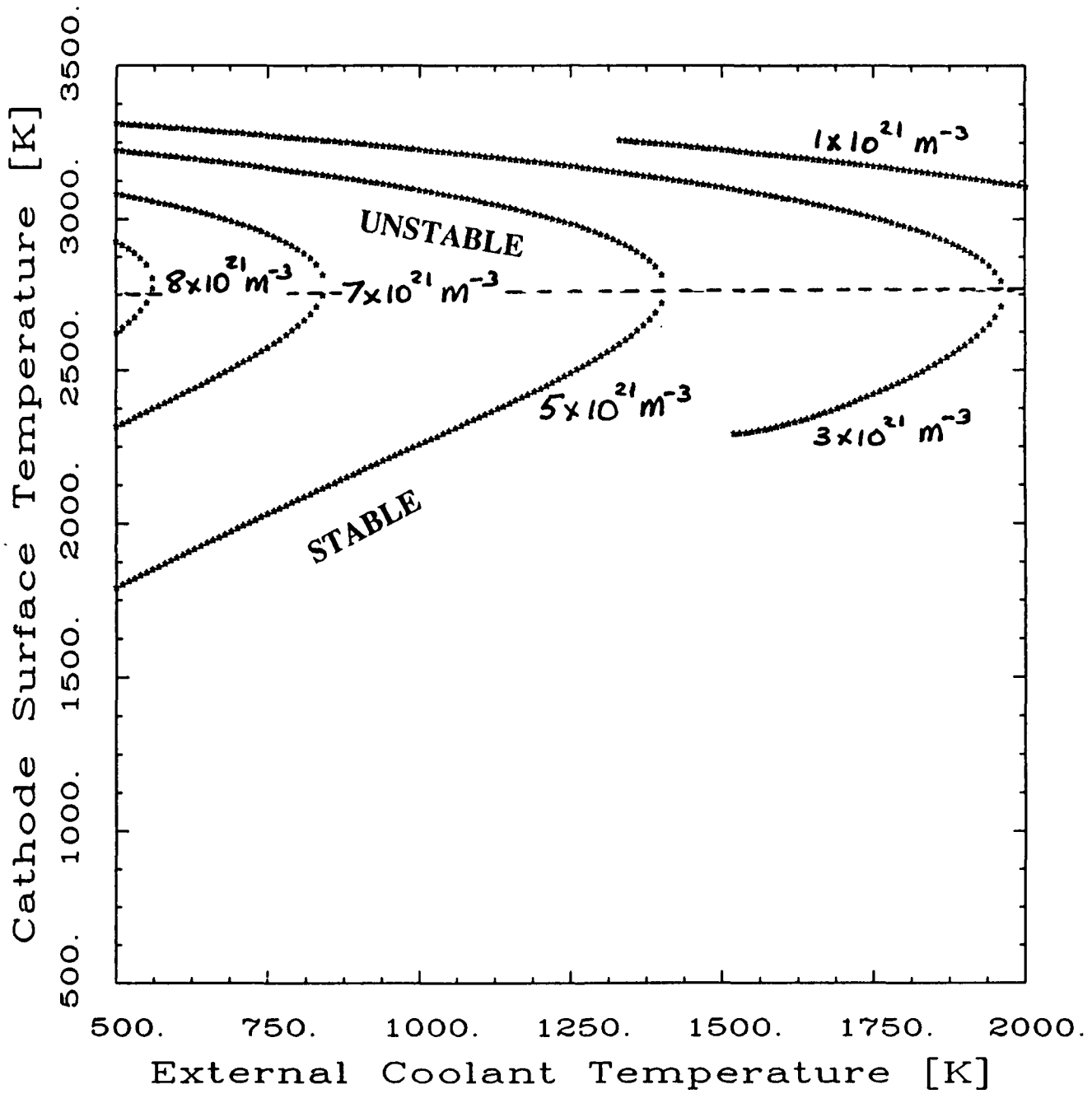
Cathode Surface Temperature [K]
500.
1000.
1500.
2000.
2500.
3000.
3500.
500.
750.
1000.
1250.
1500.
1750.
2000.
External Coolant Temperature [K]
UNSTABLE
STABLE
1x10^21 m^-3
8x10^21 m^-3
7x10^21 m^-3
5x10^21 m^-3
3x10^21 m^-3

Fig. 6

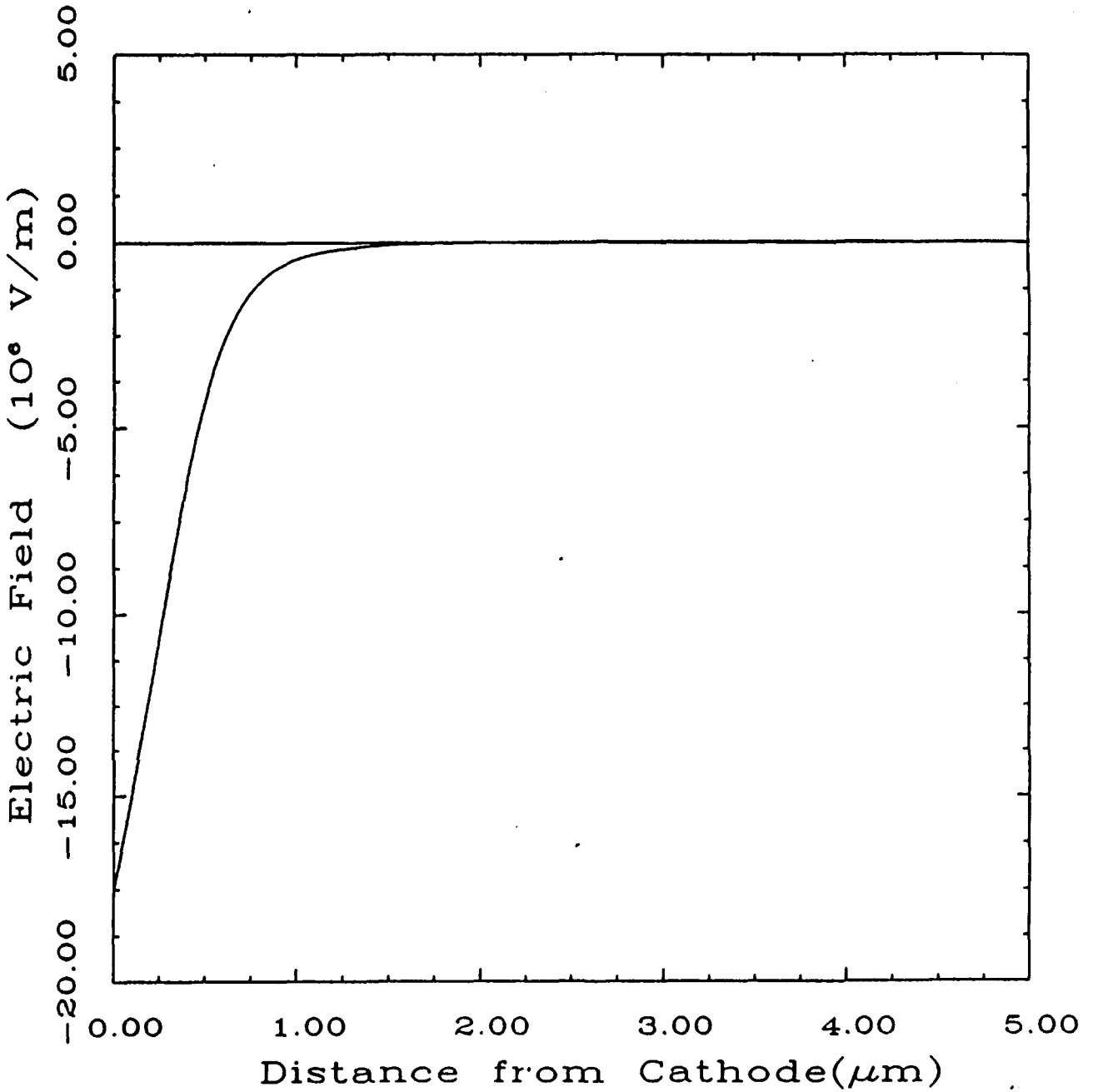
Electric Field (10⁶ V/m)
5.00
0.00
-5.00
-10.00
-15.00
-20.00
0.00
1.00
2.00
3.00
4.00
5.00
Distance from Cathode(μm)

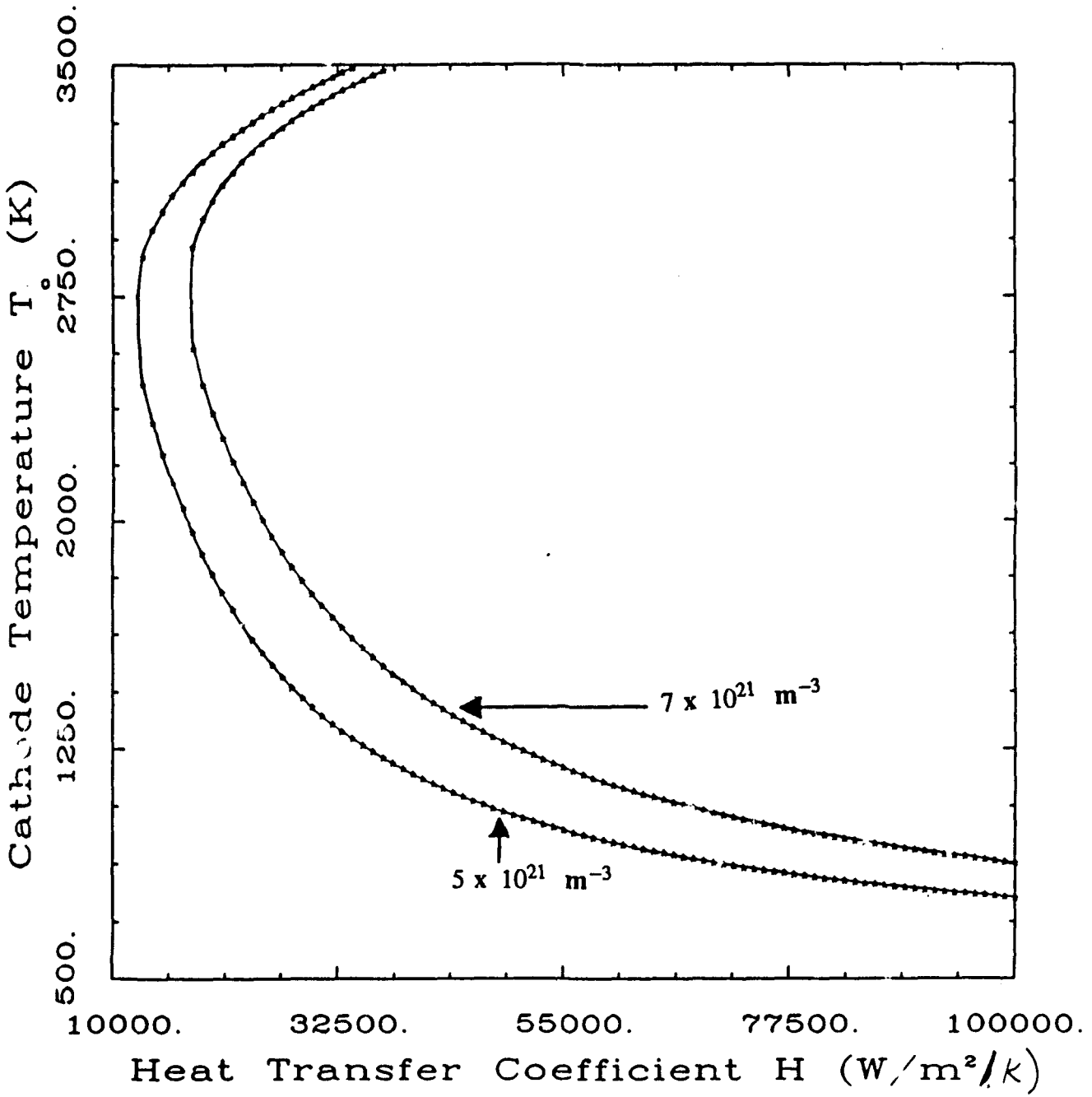
Cathode Temperature T (K)
3500.
2750.
2000.
1250.
500.
10000.
32500.
55000.
77500.
100000.
Heat Transfer Coefficient H (W/m²/k)
7 x 10²¹ m⁻³
5 x 10²¹ m⁻³

Thermal Instabilities of the Anode in a Magnetoplasmadynamic Thruster

V. V. Subramaniam*
Ohio State University, Columbus, Ohio
and
J. L. Lawless†
Space Power Inc., San Jose, California

Nomenclature

A = thermionic emission coefficient
d = anode thickness
e = electronic charge
J = total current
j = current density passing through the anode
j_e = electron current density from the plasma (Its sense is positive away from the anode.)
j_E = current density of thermionically emitted electrons (Its sense is positive into the anode.)
j_∞ = average net current density through the plasma, taken positive away from the anode
k = Boltzmann's constant
L = anode length
m_e = electron mass
n_e = electron number density at the plasma-sheath boundary
$O(\ )$ = order of magnitude of the quantity in parenthesis
q_0 = heat flux on the anode inner surface (Its sense is positive into the anode surface.)
T = temperature
T_0 = anode inner surface temperature
T_{0c} = critical value of T_0 where $\partial j_\infty/\partial T_0 = 0$
T_d = anode outer surface temperature
T_e = plasma electron temperature
V_A = anode sheath voltage drop, defined as the potential at the plasma-sheath edge minus the anode potential
W = anode width
x = outward coordinate taken to be 0 at the anode inner surface, and d at the anode outer surface
ϵ = emissivity of outer anode surface
λ = thermal conductivity of anode material
σ_{SB} = Stefan-Boltzmann constant
σ = electrical conductivity of anode material
Φ_A = anode material work function

I. Introduction

An important consideration in the use of magnetoplasmadynamic (MPD) thrusters operating at steady state for space missions is electrode erosion. Erosion in MPD thrusters has been studied experimentally and has focused mainly on the cathode.[1-3] There are also ongoing experiments in cathode erosion.[4] However, in this article, we present a simple analysis of the energy balance on the anode in an effort to predict anode surface temperatures. This can subsequently be used to predict erosion rates by evaporation. As will be shown, even such a simple model reveals subtle physical phenomena.

Electrode erosion is connected with the modes of current conduction through the electrode surface. Two modes are known to exist: spot and diffuse. The diffuse mode at subonset conditions is the focus of this article. Vainberg et al.[5] have considered anode behavior at onset conditions and beyond. Their explanation of anode melting rests on the anode sheath reversal mechanism which has also been observed by Hugel.[6] In constrast to these earlier works, it is shown in this article that a thermal runaway may occur well *before* the sheath reversal. This work supports earlier conjectures that local surface melting of the anode precedes spot formation.[7] Two operating modes are predicted by the theory presented here. One of these yields a stable steady-state temperature for the anode, whereas the other results in a thermal runaway in which the anode regeneratively heats itself until it melts. The total current, anode geometry, and material work function are shown to strongly influence the steady-state anode temperature for the stable operating regime.

In the following section, the governing equations describing anode heat transfer will be derived. The solutions to these equations under some conditions of interest are given and discussed in Sec. III, followed by the summary and conclusions in Sec. IV.

II. Anode Energy Balance

Consider the hollow cylindrical anode geometry of the MPD thruster modeled as a long thin slab of length L, width W, and thickness d (shown in Fig. 1). At steady state, the energy balance gives

$$\lambda \frac{d^2T}{dx^2} = -\frac{j^2}{\sigma} \tag{1}$$

Equation (1) is subjected to the following boundary conditions:

$$-\lambda \frac{dT}{dx}\Big|_{x=0} = q_0 \tag{2}$$

$$-\lambda \frac{dT}{dx}\Big|_{x=d} = \epsilon \sigma_{SB} T_d^4 \tag{3}$$

For the case of constant properties, the system of Eqs. (1-3) may be readily integrated to give

$$\epsilon \sigma_{SB} T_d^4 = \frac{j^2 d}{\sigma} + q_0 \tag{4}$$

and

$$\lambda T_d = -\frac{j^2 d^2}{2\sigma} - q_0 d + \lambda T_0 \tag{5}$$

Received Feb. 22, 1988; revision received Oct. 3, 1988.

*Assistant Professor. Member AIAA.
†Senior Scientist and Manager of Advanced Concepts. Member AIAA.

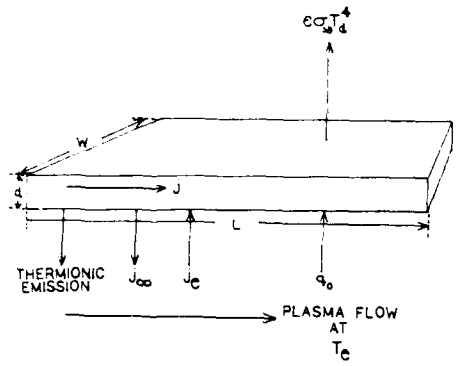

Fig. 1 The hollow cylindrical anode is shown in this idealization as a long thin slab of length L, width W, and thickness d.

Now, if q_0 is known and j is given, Eqs. (4) and (5) represent two equations for the two unknowns T_0 and T_d.

The heat flux on the anode inner surface q_0 must be found by considering particle bombardment from the plasma through the sheath. Consider, therefore, a power balance per unit area on the anode inner surface. The focus here is on conditions prior to sheath reversal; therefore, the anode is at a lower potential with respect to the plasma potential at the sheath edge. The power balance, then, mainly consists of a balance between electron bombardment and thermionic emission cooling. It can be shown that under these operating conditions evaporative cooling is a relatively small effect. Ion bombardment may be easily included in our analysis, but we neglect it for simplicity. Although this is expected to influence final results quantitatively, the conclusions regarding the mechanisms responsible for a thermal runaway will not be altered. We then have

$$q_0 = j_e(\phi_A + 2kT_e/e) - AT_0^2 \times (\phi_A + 2kT_0/e)\exp\{-e\phi_A/kT_0\} \tag{6}$$

The electron current density from the plasma j_e can be determined from overall current conservation

$$j_e = j_\infty + AT_0^2 \exp\{-e\phi_A/kT_0\} \tag{7}$$

Inclusion of ion bombardment would involve additional terms on the right hand side of Eqs. (6) and (7). The anode sheath drop may be determined from Eq. (7) to be

$$V_A = -\frac{kT_e}{e}\ln[(j_\infty + j_E)/j_r] \tag{8}$$

where $j_r = en_e(kT_e/2\pi m_e)^{\frac{1}{2}}$ and $j_E = AT_0^2 \exp\{-e\phi_A/kT_0\}$. The anode is at a potential of $-V_A$ with respect to the plasma-sheath edge (taken as the $V=0$ datum) in the regime under consideration. Combining Eqs. (6) and (7) gives

$$q_0 = j_\infty\left(\phi_A + \frac{2kT_e}{e}\right) + \frac{2AkT_0^2(T_e - T_0)}{e}\exp\{-e\phi_A/kT_0\} \tag{9}$$

Finally, combining Eqs. (4) and (5), we get an implicit equation for T_0

$$F(T_0) = \frac{j^2 d}{\sigma} + q_0 - \epsilon\sigma_{SB}\left(T_0 - \frac{q_0 d}{\lambda} - \frac{j^2 d^2}{2\lambda\sigma}\right)^4 = 0 \tag{10}$$

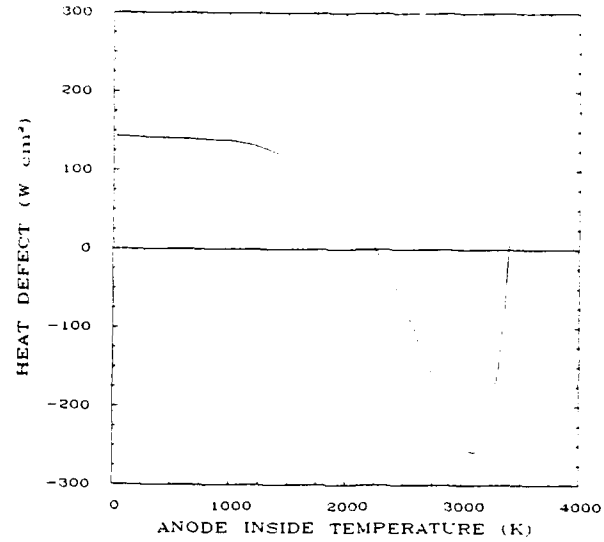

Fig. 2 A typical variation of the heat defect (defined as the net heat flux into the anode minus the net heat flux out) is shown here vs the anode inside surface temperature T_0.

where q_0 is given by Eq. (9). Given d, L, W, T_e, and J, the axial current density throught the anode ranges up to $j = J/Wd$, and the average current density through the plasma at the anode surface is $j_\infty = J/WL$. Although this simplification is unnecessary (since j and j_∞ can be treated as separate pointwise parameters), it allows the thermal steady state to be related directly to the total current (a more tangible quantity) rather than the current densities. With these quantities, Eq. (10) may be solved for T_0. Once T_0 is determined, T_d may be readily obtained from Eqs. (4) or (5). Equations (9) and (10) have been solved in this manner for representative conditions in the MPD thruster. These results are discussed in the following section.

III. Analysis and Results

In the previous section, it was shown that an energy balance on the anode at steady state yields an implicit equation for the anode inside the surface temperature T_0. This equation [Eq. (10)] is nonlinear in T_0 and must be solved numerically. This section will focus on the solution of this implicit equation, resulting in the discovery of a thermal runaway mode and culminating in a discussion of various operating limits.

For illustrative purposes, let us consider a tungsten anode of width 30 cm and length 10 cm. Let the electron temperature T_e be fixed at 15,000 K. The typical variation of the implicit function $F(T_0)$ vs T_0, given by Eq. (10), is displayed in Fig. 2. The function $F(T_0)$ represents the net heat into the anode per unit area per unit time. It is immediately evident from Fig. 2 that two steady-state solutions exist. Without performing a stability analysis, one can conclude on the basis of physical reasoning that the lower temperature is a stable root and the higher one is an unstable root. Consider the smaller temperature first. Any perturbation to the left of this root (i.e., on the lower temperature side) results in a net heat flux into the anode. To counter this, the surface temperature must increase in order to maintain a steady state. Similarly, any small perturbation to the right (i.e., on the higher temperature side) results in a net heat flux out of the anode. To counter this, the surface temperature must decrease. Thus, we see that the tendency of the thermal response is to drive the temperature toward this root. Using this physical argument on the second root (i.e., higher temperature), we may conclude that it is unstable. If the surface temperature increases just above the value given by the second root, the steady-state energy balance indicates a further increase in temperature in order to maintain a steady state. This is because the only possible way of losing energy is through radiation and by thermionic emission,

both of which increase with increasing temperature. This results in a thermal runaway with eventual melting of the anode.

A physical interpretation of the two aforementioned solutions will now be discussed. Examination of Eq. (8) indicates that the anode sheath drop decreases as the net plasma current density increases. This results in increased electron bombardment, as can be seen from Eqs. (6) and (7), causing heating of the anode surface. Two possible scenarios may ensue. The resulting increase in the surface temperature leads to an increase in the emission current density, which further lowers the anode sheath voltage drop. This positive feedback may repeat itself until thermal runaway leads to local melting of the surface. The second scenario is stable, steady operation arising from the fact that sufficient cooling of the anode prevents the thermal runaway by excessive electron bombardment. The two solutions found to Eq. (10) represent these two situations.

The anode surface temperature T_0 for stable operation is found to be strongly dependent on the total current, anode geometry, and the anode work function. Figure 3 shows the anode thickness for various total currents, and Fig. 4 shows the anode inside surface temperature vs total current for various anode thicknesses. From these results, it is evident that for a given total current, there exists an optimum thickness for achieving a minimum anode temperature. An interesting feature of the pair of solutions found to the steady-state heat balance equation is that the stable and unstable roots start moving toward each other as the current is increased. This continues until a critical value of the current is reached, beyond which no steady solution can be found below the melting point of the material. Also, for a fixed total current, these roots approach each other as the thickness is increased. It is possible that the analytical behavior of this unstable thermal runaway point will yield insight into electrode material breakdown.

Some interesting limits may be readily obtained by analyzing the equations presented in Sec. II. For instance, from Eq. (5) it is clear that

$$j^2d^2/2\sigma < kT_0 \quad \text{or} \quad j < j_c = (2k\sigma T_0)^{1/2}/d \tag{11}$$

which is very similar (within a proportionality constant) to the thermal runaway condition obtained by Hantzsche[8] for cathode spots. However, it must be pointed out that Eq. (11) is obtained here for an anode of constant electrical conductivity, operating in the diffuse mode. This sharply differs from Hantzsche's consideration of a cathode spot with an electrical conductivity that varies according to the Wiedemann-Franz law (i.e., $\sigma \propto 1/T$). Furthermore, in constrast to Hantzsche's work, surface cooling due to thermionic emission *does not* prevent thermal runaway. This thermal runaway can occur under the steady, diffuse mode operation of the anode.

An important stability criterion may be derived by requiring that $\delta F/\delta T_0 < 0$ for stable diffuse operation. Using Eq. 7, we find

$$V_A \geq \frac{-kT_e}{e} \ell n \left[\frac{j_\infty + 0\left(\frac{4\epsilon J_{SB} T_d^3 T_0^2}{2\phi_A T_e}\right)}{j_r} \right] \tag{12}$$

For V_A below the value given by the right-hand side of Eq. (12), excessive electron bombardment will cause a thermal runaway. Thus, local surface melting can occur prior to sheath reversal.

A limit may also be found for the plasma current density j_∞. Considering thin anodes (i.e., $T \approx T_0$ throughout the anode), neglecting ohmic heating and any external cooling except for radiation, we may write the energy balance at steady state as

$$\epsilon\sigma_{SB}T_0^4 = j_\infty\left(\phi_A + \frac{2kT_e}{e}\right) + \frac{2kAT_0^2}{e}(T_e - T_0)\exp(-e\phi_A/kT_0) \tag{13}$$

Using the fact that $T_e \gg T_0$, differentiating with respect to T_0, and setting $\partial j_\infty/\partial T_0 = 0$, we obtain

$$(j_\infty)_{max} \approx \frac{[1-(4kT_{0c}/e\phi_A)]}{[\phi_A + (2kT_e/e)]}\epsilon\sigma_{SB}T_{0c}^4 \tag{14}$$

where $(j_\infty)_{max}$ is the extremum plasma current density, and T_{0c} is the critical value of T_0 where $\partial j_\infty/\partial T_0 = 0$. Additional heat transfer to an external coolant results only in a slight modification of Eq. (14):

$$(j_\infty)_{max} \approx \frac{[1-(4kT_{0c}/e\phi_A)]}{[\phi_A + (2kT_e/e)]}\epsilon\sigma_{SB}T_{0c}^4 + \frac{[1-(kT_{0c}/e\phi_A)]}{[\phi_A + (2kT_e/e)]}hT_{0c} \tag{15}$$

where h is the heat transfer coefficient between the anode (at T_0) and an external coolant (at $T_c \ll T_0$). For $T_e = 20{,}000$ K, Eq. (14) approximately yields 47.6 A/cm^2 for a tungsten anode ($\phi_A = 4.52$ V) and 5.4 A/cm^2 for a thoriated tungsten anode ($\phi_A = 2.63$ V). The lower work function yields a lower maximum plasma current density because of a lower value of T_{0c}. Since these limiting current densities are far lower than

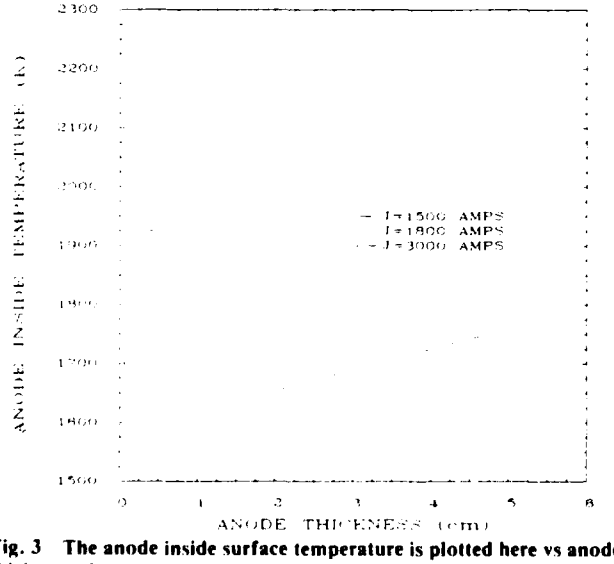

Fig. 3 The anode inside surface temperature is plotted here vs anode thickness, for various total currents.

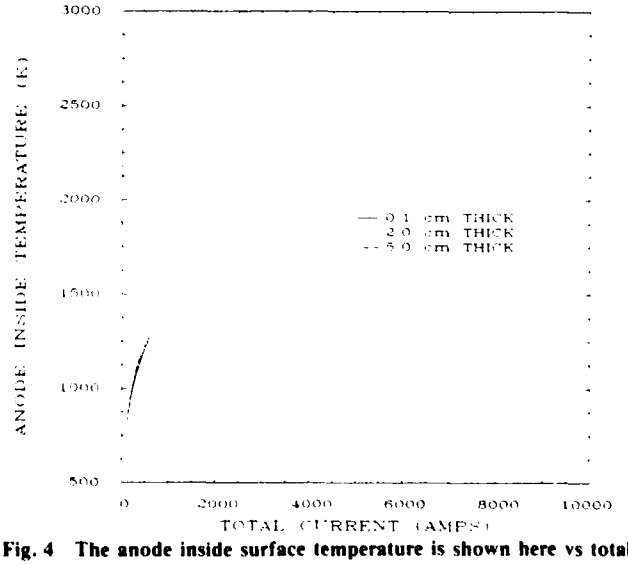

Fig. 4 The anode inside surface temperature is shown here vs total current, for various anode thicknesses.

those required for a steady MPD discharge, it is clear that the anode must be cooled externally. This is done in practice.[1,4]

IV. Summary and Conclusions

An anode energy balance has been performed that includes the effects of the anode sheath. Results show that under many conditions, two steady-state solutions can be found. One of these corresponds to a stable operating point, the other to a thermal runaway. The stable root that gives the anode inside surface temperature at steady state was found to be strongly dependent on the total current, anode geometry, and the material work function. A stability condition in the form of a minimum anode sheath voltage drop [Eq. (12)] has also been given.

Several conclusions can be derived from the anode thermal analysis:

1) There exists, for a given current density, an optimum thickness for achieving a minimum anode temperature.

2) Under many conditions, there exists a pair of steady-state solutions to the heat balance, one of which is a stable operating point, the other of which is an unstable thermal runaway point.

3) There exists a maximum steady operating current density for a given electrode geometry based on melting temperature and cooling considerations.

The thermal runaway mode discovered for the anode may explain anode spots under MPD conditions. Although some limits have been found, anode heat transfer effects need to be explored further in order to learn more about what controls the limits of stable operation. Since external cooling is seen to be extremely important, detailed experimental results quantifying cooling rates for various operating conditions and geometries would be valuable. Radiative heat transfer from the plasma, which has been neglected here, is another important area for further research.

Acknowledgments

This work was supported by AFOSR-83-0033 and by AFOSR-87-0360. The authors acknowledge helpful discussions with D. Q. King.

References

[1]Kurtz, H. L., Auweter-Kurtz, M., and Schrade, H. O., "Self-Field MPD Thruster Design—Experimental and Theoretical Investigations," AIAA Paper 85-2002, Alexandria, VA, Sept.-Oct. 1985.

[2]Schrade, H. O., Auweter-Kurtz, M., and Kurtz, H. L., "Cathode Erosion Studies on MPD Thrusters," *AIAA Journal*, Vol. 25, Aug. 1987, pp. 1105-1112.

[3]Harstad, K., "Electrode Processes in MPD Thrusters," Jet Propulsion Laboratory Publication 81-114, March 1982.

[4]King, D. Q., private communication, Nov. 18, 1987.

[5]Vainberg, L. I., Lyubimov, G. A., and Smolin, G. G., "High-current Discharge Effects and Anode Damage in an End-Fire Plasma Accelerator," *Soviet Physics Technical Physics*, Vol. 23, April 1978, pp. 439-443.

[6]Hugel, H., "Effect of Self-Magnetic Forces on the Anode Mechanism of a High Current Discharge," *IEEE Transactions on Plasma Science*, Vol. PS-8, No. 4, Dec. 1980.

[7]Miller, H. C., "Vacuum Arc Anode Phenomena," *IEEE Transactions on Plasma Science*, Vol. PS-11, No. 2, June 1983.

[8]Hantzsche, E., "Thermal Runaway Prevention in Arc Spots," *IEEE Transactions on Plasma Science*, Vol. PS-11, No. 3, Sept. 1983.